An integrated analysis of an orogen–sedimentary basin pair: Latest Cretaceous–Cenozoic evolution of the linked Eastern Cordillera orogen and the Llanos foreland basin of Colombia

German Bayona[†]
Smithsonian Tropical Research Institute, Unit 0948, APO AA 34002-0948, USA, and *Corporación Geológica ARES, Calle 57 No. 24-11 of 202, Bogotá, Colombia*

Martin Cortés
Corporacón Geológica ARES, Calle 57 No. 24-11 of 202, Bogotá, Colombia

Carlos Jaramillo
Smithsonian Tropical Research Institute, Unit 0948, APO AA 34002-0948, USA

German Ojeda
Instituto Colombiano del Petróleo, AA 41815, Km 7 to Piedecuesta, Bucaramanga, Colombia

John Jairo Aristizabal[§]
Ecopetrol S.A., Calle 37 No. 8-43, Bogotá, Colombia

Andres Reyes-Harker
Instituto Colombiano del Petróleo, AA 41815, Km 7 to Piedecuesta, Bucaramanga, Colombia

ABSTRACT

The integration of restored basin geometry and internal features of syntectonic units (e.g., stratal architecture, thickness, sandstone composition) with flexural modeling of the lithosphere constrains the evolution of a basin and its flexural history related to orogenic growth (spatial/temporal loading configuration). Using this approach, we determined the Maastrichtian-Cenozoic polyphase growth of the Eastern Cordillera of Colombia, an inverted Mesozoic extensional basin. The record of this growth occurs in an Andean (post–middle Miocene) thrust belt (the Eastern Cordillera) and in adjacent foreland basins, such as the Llanos Basin to the east. This approach permitted the identification of five tectono-stratigraphic sequences in the foreland basin and five phases of shortening for the Eastern Cordillera. Thermochronological and geochronological data support the spatial and temporal evolution of the orogen–foreland basin pair.

Tectono-stratigraphic sequences were identified in two restored cross sections, one located at a salient and the other in a recess on the eastern flank of the Eastern Cordillera. The lower two sequences correspond to late Maastrichtian–Paleocene flexural events and record the eastward migration of both tectonic loading and depositional zero in the Llanos Basin. These sequences consist of amalgamated quartzarenites that abruptly grade upward to organic-rich fine-grained beds and, to the top, light-colored mudstones interbedded with litharenites in isolated channels. Amalgamated conglomeratic quartzose sandstones of the third sequence record ~15 m.y. of slow subsidence in the Llanos Basin and Llanos foothills during early to middle Eocene time, while shortening was taking place farther west in the Magdalena Valley. The fourth sequence, of late Eocene–middle Miocene age, records a new episode of eastward migration of tectonic loads and depositional zero in the Llanos Basin. This sequence begins with deposition of thick fine-grained strata to the west, whereas to the east, in the Llanos basin, amalgamated quartzarenites unconformably overlie Cretaceous and older rocks (former forebulge). Apatite fission tracks in the axial zone of the Eastern Cordillera, growth strata in the Llanos foothills, and synextensional strata on the forebulge of the Llanos Basin constrain deformation patterns for this time. The post–middle Miocene Andean event initiated with regional flooding of the foreland basin in response the widening of tectonic loading, after which the foredeep was filled with coarse-grained alluvial and fluvial detritus derived from the Eastern Cordillera.

The geometry of tectonic loads, constrained by flexural models, reveals shortening events of greater magnitude for the uppermost two sequences than for pre–middle Eocene sequences. Tectonic loads for the late Maastrichtian–middle Eocene phases of shortening were less than 3 km high and 100 km wide. For the late Eocene–middle Miocene phase, tectonic loads changed southward from 6 km to less than 4 km, and loads were wider to the north. The strong Andean inversion formed today's Eastern Cordillera structural configuration and had equivalent tectonic loads of 10–11 km.

Integrated analysis is necessary in polyphase orogenic belts to define the spatial and temporal variation of tectonic load and foreland basin configurations and to serve studies that seek to quantify exhumation and three-dimensional analyses of thrust belts. For the

[†]E-mail: gbayona@cgares.org
[§]Present address: REPSOLYP, Calle 71A No. 5-38, Bogotá, Colombia.

GSA Bulletin; September/October 2008; v. 120; no. 9/10; p. 1171–1197; doi: 10.1130/B26187.1; 15 figures; Data Repository item 2008078.

Eastern Cordillera, thermochronological sampling must span the width of the Eastern Cordillera rather than be concentrated in a single range.

Keywords: foreland basin, Cenozoic stratigraphy, basin inversion, orogenic belts, Cenozoic tectonics, Llanos Basin, Colombia.

INTRODUCTION

Integrative research on syntectonic sedimentary basins should include different types of data sets (sedimentology, stratal architecture, provenance, subsidence) and needs to consider kinematic constraints from the adjacent mountain belts. Tectonic activity, weathering processes, and isostatic readjustment of the crust delimit uplifted blocks and so determine the nature of crustal loads adjacent to a basin. On the other hand, syntectonic sedimentary basins include the most complete record of the evolution of those uplifted blocks. Initiation of deformation in a formerly tectonically quiet (e.g., passive margin) and nearly flat (e.g., coastal plain) region affects depositional and paleoecological systems, provenance, and paleocurrent indicators, as well as climate variables (e.g., precipitation). The rearrangement of these variables influences the tectonic evolution of both mountain ranges (e.g., climatic control of critical wedge in the central Andes; Horton, 1999) and adjacent sedimentary basins (e.g., change in fluvial patterns of the Amazon Basin by uplift of the Andes; e.g., Hoorn et al., 1995).

The kinematic evolution of an orogen affects both the geometry and filling patterns of syntectonic sedimentary basins. In orogen and foreland basin systems, estimates of spatial and temporal variations of crustal thickening commonly rely on studies of orogenic belt deformation in conjunction with proximal-to-distal synorogenic stratigraphic and compositional analyses (e.g., Horton et al., 2001; Liu et al., 2005) of the foreland basin. Geodynamic models of foreland basins have been essential in defining the spatial and temporal variation of tectonic load geometries, since there is a primary relationship among tectonic loading, strength of the lithosphere, and basin geometry (e.g., Jordan, 1981; Cardozo and Jordan, 2001).

Integrated orogen and foreland basin analysis of the type presented here is an essential approach to understanding of polyphase thrust-belt systems and deciphering deformation phases. Investigations in the central (e.g., Horton et al., 2001) and northern Andes (e.g., Gómez et al., 2005a) indicate that pre-Neogene deformation played an important role in the tectonic evolution of the Andes, which are believed to have risen strongly in the late Neogene. Therefore, studies of shortening in the Eastern Cordillera of Colombia, a mountain range of the northern Andes, must consider temporal and spatial variations of crustal shortening that resulted from pre-Neogene phases of deformation.

This paper presents a kinematic evolution and quantification of tectonic loading of a polyphase-deformed orogenic belt (Eastern Cordillera) adjacent to a nonmarine foreland basin (Llanos Basin). We integrate provenance, sedimentology, stratal patterns, biostratigraphy, subsidence, structural, and geodynamic analyses with published thermochronological and geochronological data in order to (1) investigate how crustal thickening (i.e., tectonic loading) affected the latest Cretaceous–Paleogene evolution of the Llanos foreland basin, and (2) identify structures in the Eastern Cordillera that might have been active at each phase of deformation. Our results suggest that the present topography of the Eastern Cordillera does not reflect the complex earlier evolution of the northern Andes but rather provides a record only of the last phase of deformation. Therefore, integrated analysis of the adjacent Llanos foreland basin is necessary to investigate the previous deformation events, which are masked by the last phase.

TECTONIC FRAMEWORK OF THE COLOMBIAN ANDES AND EVIDENCES OF PRE-NEOGENE DEFORMATION

Regional Tectonic Setting of the Eastern Cordillera

Three major orogenic belts are the result of the complex interaction of the Nazca, Caribbean, and South America plates since the Late Cretaceous: the Western Cordillera, the Central Cordillera, and the Eastern Cordillera. The Eastern Cordillera bifurcates to the north into the Santander massif–Perija Range (MS-PR) and the Merida Andes (MA) (Fig. 1). The Eastern Cordillera is interpreted as a wide Cretaceous extensional basin that was formed during at least two stretching events (Sarmiento-Rojas et al., 2006) and that was tectonically inverted during the Cenozoic (Colleta et al., 1990; Dengo and Covey, 1993; Cooper et al., 1995; Mora et al., 2006). However, basement and sedimentary rocks exposed in the Eastern Cordillera and adjacent basins indicate that this complex region has been the scene of polyphase tectonics since Precambrian time (see Etayo-Serna et al. [1983] and Cediel et al. [2003] for details).

The eastern flank of the Eastern Cordillera of Colombia (Fig. 1) exposes contrasting structural styles between highly deformed rocks along an east-verging fold-and-thrust belt and the less-deformed Llanos foreland basin. Reactivated Mesozoic normal faults, such as the Guaicaramo fault system in the central Llanos foothills, have been considered to be the major boundary of those structural styles. Models of inversion tectonics have been created for the southern segment of the Eastern Cordillera and Llanos foothills (Casero et al., 1997; Rowan and Linares, 2000; Branquet et al., 2002; Restrepo-Pace et al., 2004; Toro et al., 2004; Cortés et al., 2006a; Mora et al., 2006), in the central segment of the Eastern Cordillera and Llanos foothills (Colleta et al., 1990; Dengo and Covey, 1993; Cooper et al., 1995; Cazier et al., 1995; Roeder and Chamberlain, 1995; Rathke and Coral, 1997; Fajardo-Peña, 1998; Taboada et al., 2000; Sarmiento-Rojas, 2001; Rochat et al., 2003; Toro et al., 2004; Martinez, 2006; Mora et al., 2006), and in the northern segment of the Eastern Cordillera and Llanos foothills (Chigne et al., 1997; Corredor, 2003; Villamil et al., 2004). Although structural models differ both in the angle and depth of detachment of the Guaicaramo fault system and in fault involvement of crystalline basement to the east, structural restorations from the axial zone of the Eastern Cordillera and Llanos Basin are similar (Fig. 1C). Proposed structural models do not show a relationship between the amount of shortening and flexural deformation in the adjacent basin, and they differ in (1) the amount of shortening of the Eastern Cordillera, mainly from the axial zone to the western boundary of the Eastern Cordillera (Fig. 1C), (2) the geometry of fold structures at depth, and (3) the position and configuration of Mesozoic eastern and western rift shoulders.

As an alternative method to validate the shortening estimated in our cross sections, we used the flexural geometry of synorogenic Paleogene to Neogene foreland basins, growth-strata patterns, and crosscutting relationships of hanging-wall and footwall structures on the eastern flank of the Eastern Cordillera and Llanos foothills to better constrain the kinematic evolution of the eastern flank of the Eastern Cordillera.

Evidence of Pre-Neogene Deformation

Paleobotanical, thermochronological, and geochronological data indicate that surface and rock uplift, as well as rock deformation, have occurred at different times but primarily in the late Neogene. Paleobotanical data indicate a change in flora from lowland associations to Andean-type forests (Helmens, 1990) in the last 5 m.y., but the timing of this change ranges between 3 and 6 Ma (Helmens and Van der Hammen, 1994; Hooghiemstra and Van der Hammen, 1998). Zircon fission-track ages support earlier uplift in the Central Cordillera

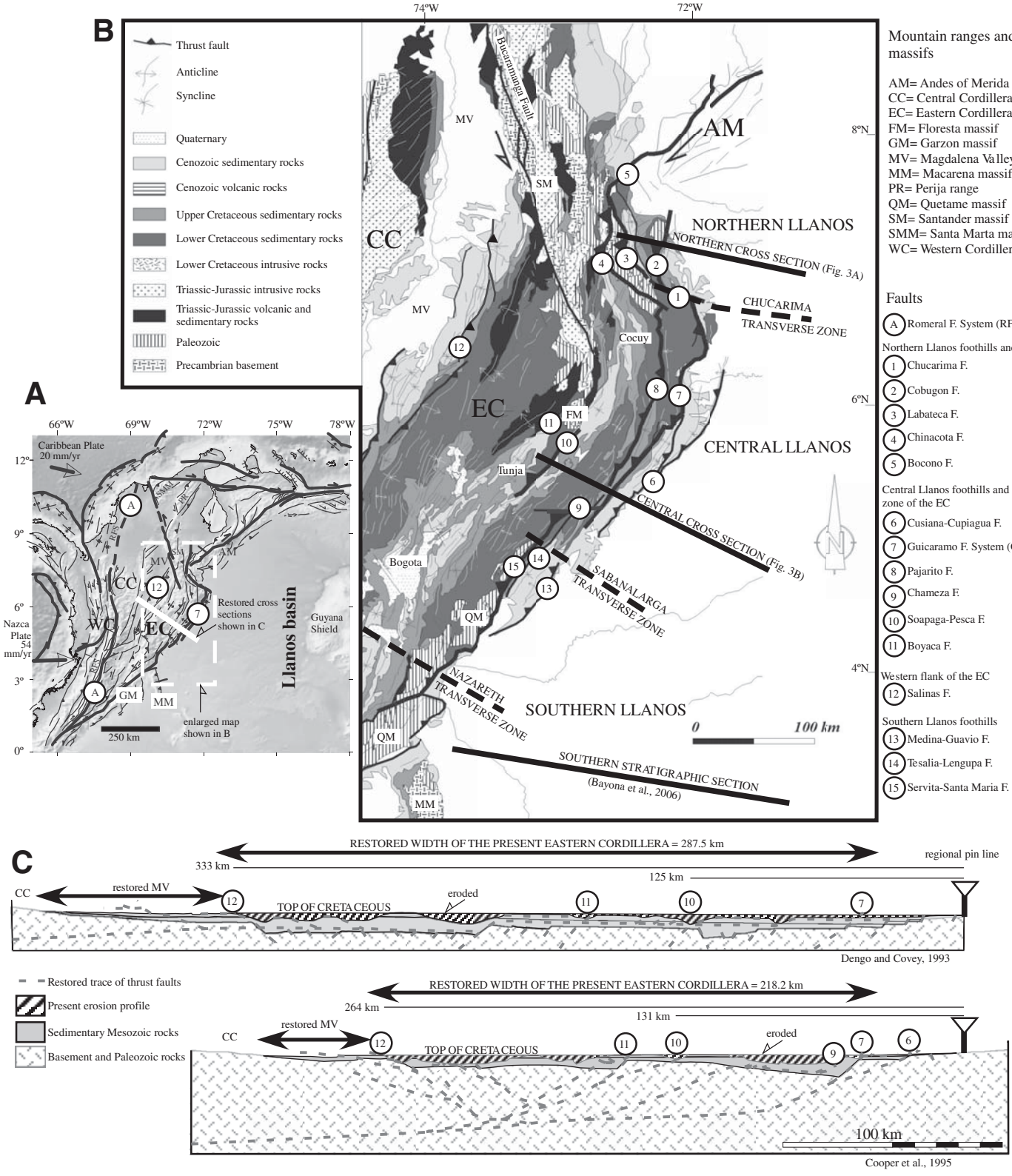

Figure 1. (A) Regional tectonic setting of the northern Andes of Colombia. (B) Geologic map of the Eastern Cordillera of Colombia (modified from Cediel and Cáceres, 1988) showing the location of the northern and central cross sections (see Fig. 3) and stratigraphic control along the southern stratigraphic cross section (for details, see Bayona et al., 2006). (C) Restored cross sections showing different interpretations of the restored position and geometry of major structures of the Eastern Cordillera. The restored distance between a regional pin line in the Llanos Basin and the Soapaga-Pesca fault (western boundary of our study area) is similar between these two interpretations (difference = 6 km). In contrast, the restored width of the western flank of the Eastern Cordillera differs by 75 km.

(around the Campanian-Maastrichtian boundary; Toro, 1999; Gómez et al., 2005a) than in the Santander massif–Perija Range and Merida Andes (near the Cretaceous-Tertiary [KT] boundary; Shagam et al., 1984; Kohn et al., 1984). Apatite fission-track ages (AFTA) indicate a northward exhumation that began in the Oligocene in the Floresta (22.3 ± 4 Ma) and southern Santander (30.8 ± 5.8 Ma) massifs (Toro, 1990), then moved to the central and northern Santander massif in the Miocene and Miocene-Pliocene, respectively (Shagam et al., 1984). AFTA ages on the western flank of the Eastern Cordillera (Gómez et al., 2003) support two phases of cooling, the first between 65 and 30 Ma, which involved the removal of 3–4 km of overlying sedimentary cover, and the second between 10 and 5 Ma, which involved denudation of 3 km of sedimentary cover. AFTA results on the eastern flank of the Eastern Cordillera (Hossack et al., 1999) require exhumation along the Chameza fault at 25 Ma and exhumation in the foothills between 3 and 15 Ma. AFTA data from the Garzon and Quetame massifs indicate younger phases of deformation, ranging from 12 to 3 Ma (Van der Wiel, 1991). The generation of an orographic barrier at ca. 6–3 Ma triggered rapid denudation and shortening rates of the eastern flank of the Eastern Cordillera (Mora et al., 2005). Reported geochronological data from green muscovite crystallized on emerald-bearing vein wall rocks (Ar/Ar and K/Ar) indicate a first extensional event at 65 ± 3 Ma on the eastern flank and a compressional event on the western flank between 32 and 38 Ma (Branquet et al., 1999).

A regional shift from marine to continental depositional environments at the end of the Cretaceous was coeval with accretion of oceanic terranes west of the Romeral fault system (e.g., Etayo-Serna et al., 1983; McCourt et al., 1984). Mechanisms driving this shift have been interpreted as eustasy and tectonism (Villamil, 1999) or increasing rate of sediment supply associated with exhumation and denudation of the Central Cordillera (Gómez et al., 2005a). Interpreted Paleocene basin geometry varies from a single and continuous foreland basin (Cooper et al., 1995; Villamil, 1999; Gómez et al., 2005a) to a continuous negative flexural basin with apparent absence of bounding thrusts (Pindell et al., 2005) to a foreland basin disrupted by uplifts along the axial zone of the basin (Fabre 1981, 1987; Sarmiento-Rojas, 2001; Pardo, 2004), the western border of the basin (Bayona et al., 2003; Restrepo-Pace et al., 2004, Cortés et al., 2006a), or at both borders of the basin (Fajardo-Peña, 1998; Villamil, 1999). The integration of basin geometry, provenance, paleocurrent, subsidence, and geodynamics analyses allows us to identify the location of loads that affected the geometry of the Paleocene foreland basin in the Llanos foothills and Llanos Basin.

Angular unconformities and growth-strata patterns of Paleogene beds place constraints on our ability to define phases of deformation. A highly variable angular unconformity between lower-to-middle Eocene strata resting upon Paleocene or older units has been well documented in the subsurface of the Magdalena Valley (Villamil et al., 1995; George et al., 1997; Pindell et al., 1998; Gómez et al., 2003, 2005b) and in outcrops (Restrepo-Pace et al., 2004). In the Magdalena Valley, structures beneath the unconformity have been interpreted as high-angle strike-slip faults (Pindell et al., 1998; Gómez et al., 2005b). Strata overlying this unconformity show a wedge of divergent growth strata of middle Eocene–lower Miocene age in the southern middle Magdalena Valley (Gómez et al., 2003) and upper Oligocene–middle Miocene age in the northern Magdalena Valley (Gómez et al., 2005b). In the axial zone of the Eastern Cordillera, the structure of the eastern flank of the Usme syncline (south of Bogotá in Fig. 1B) has been interpreted as a progressive unconformity that has been growing since the late Paleocene (Julivert, 1963). In the northern Llanos foothills and Llanos Basin, Corredor (2003) and Cortés et al. (2006b) reported growth-strata patterns in Oligocene-Miocene strata. In the central Llanos foothills, Rathke and Coral (1997) and Martinez (2006) suggested the incipient development of broad fault-related anticlines and synorogenic deposition during the Oligocene. Adjacent to leading structures of the Llanos foothills (e.g., Cusiana fault in Fig. 1), however, seismic reflectors of Oligocene and Miocene strata are parallel and generally isopachous (Toro et al., 2004). Parra et al. (2005) interpreted the westward coarsening and thickening of the Oligocene clastic wedge across a 20-km-wide syncline as the result of flexural subsidence related to the uplift of the Quetame massif.

STRUCTURE OF THE EASTERN FLANK OF THE EASTERN CORDILLERA

In order to better understand the regional geometry and lateral variations along the eastern fold-and-thrust belt of the Eastern Cordillera, two regional balanced cross sections extending from the axial zone of the Eastern Cordillera to the Llanos Basin were constructed in areas where the geometry of the Guaicaramo fault system, the internal structural configuration of the Eastern Cordillera, and the Cretaceous-Cenozoic stratigraphy differ (Figs. 1 and 2). Local cross sections were studied to the north and south of these regional cross sections in order to confirm and provide control on the lateral continuity and consistency of the regional structural models. Surface mapping, seismic-reflection profiles, gravity data, and well data constrain the construction of balanced cross sections. Stratigraphic thickness and units for each thrust sheet were provided from the tectono-stratigraphic analysis carried out along these regional cross sections (see next section).

Structure of the Northern Cross Section

This cross section (Fig. 3A) traverses a basement structural high, named the Pamplona indenter by Boinet et al. (1985), which is bordered by the northwest-striking Chucarima fault, north-striking Labateca and Chinacota reverse faults, and northeast-striking right-lateral Bocono fault. This cross section, located at the recess of the Guaicaramo fault system (the Guaicaramo fault system is displaced to the west to become the Cobugon fault), starts at the western flank of the Santander massif, passes through the northern Llanos foothills, and ends at the Caño Limon oil field in the northern Llanos Basin (Figs. 1 and 3A). The trace of this cross section is far from the transverse boundaries of the Pamplona indenter and at the place where deformation is mostly plane strain.

Structural domains in the Eastern Cordillera and Llanos foothills of the northern cross section involve basement rocks. These domains end southward at the northwest-striking Chucarima fault system. The latter structure places a >3-km-thick succession of lower Cretaceous rocks (Fabre, 1987) in the upthrown block over NNW-striking folds involving upper Cretaceous and Paleogene strata in the downthrown block. In the latter block, the maximum thickness of the lower Cretaceous rocks is 1.2 km (Fig. 2). South of the Chucarima fault, structural domains are more similar to those described for the central cross section.

Structural balance of the northern cross section indicates a total shortening of 30.5 km (Fig. 3A). Major basement-involved faults form the boundaries between structural domains. The west-dipping basement-involved faults translated displacement and strain eastward through an imbricated fold-and-thrust belt. The major displacements occurred along faults exposed toward the hinterland, where the Santander massif is exposed (domains DN1&2, Fig. 3A). Out-of-sequence deformation along the Cobugon and Samore faults is inferred from the crosscutting relation between fault surfaces and footwall structures (domain DN3). A late Oligocene–early Miocene phase of east-verging deformation is constrained by growth-strata patterns identified in the syncline bounded by the Samore

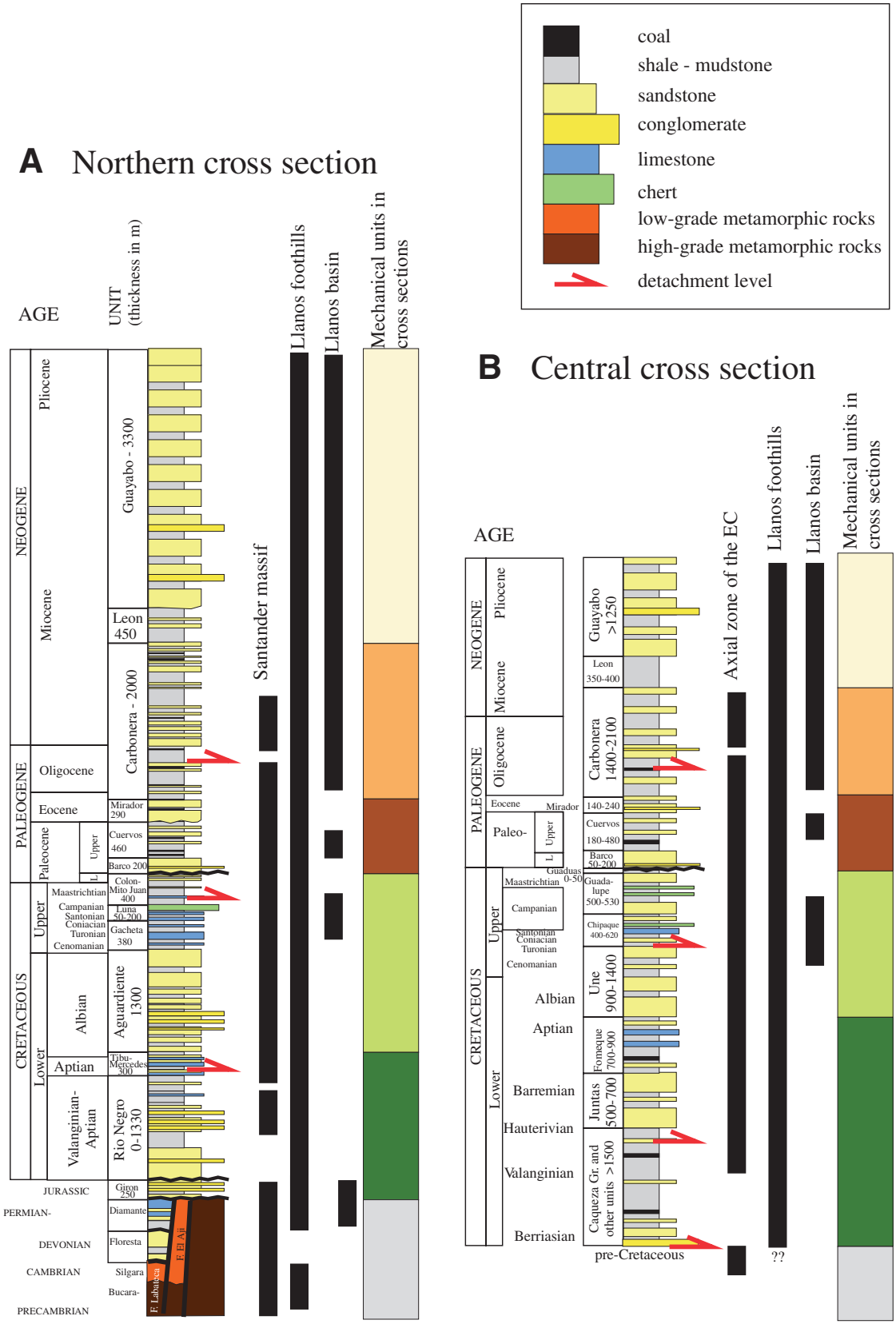

Figure 2. Generalized stratigraphic columns showing the lateral distribution of units along the (A) northern and (B) central cross sections. Regional detachment levels and mechanical units used for construction of cross sections are indicated.

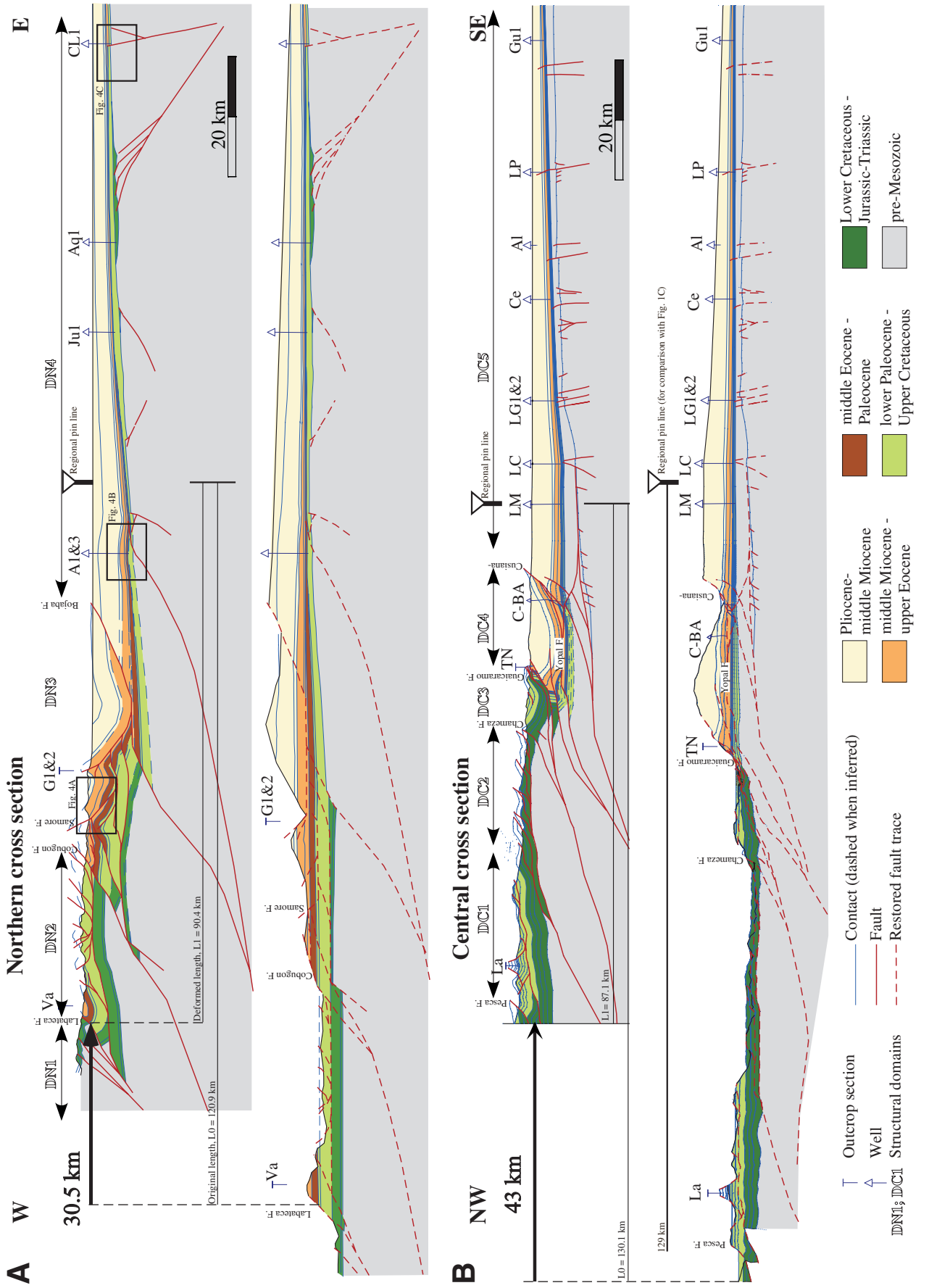

Figure 3. (A) Northern and (B) central balanced and restored cross sections showing major structures and structural domains. The amount of restoration for the eastern flank of the Eastern Cordillera along the central cross section (Fig. 3B) has similar results to those shown in Figure 1C (129 km); however, the structural geometry is more similar to the Cooper et al. (1995) interpretation. Structure of the basement in the Llanos Basin for the central cross section was modified from Geoconsult-Pangea (2003). A complete list of references for surface and subsurface data is in Cortes et al. (2006).

fault (Cortés et al., 2006b) (Fig. 4A). Two contrasting structural styles are well defined in both extremes of the northern Llanos Basin (domain DN4). In the western extreme, strata are folded in a compressive anticline structure (well A1&3 in Fig. 3A), and upper Oligocene–lower Miocene strata thin at the crest of the fold, suggesting a growth structure (Fig. 4B). At the eastern side (well CL1 in Fig. 3A), synfaulting upper Oligocene–lower Miocene strata document normal faulting (Fig. 4C). This is interpreted as flexural deformation associated with a forebulge (Cortés et al., 2006b).

The recess geometry of the frontal thrust belt north of the transversal Chucarima fault suggests that: (1) the Chucarima fault, a transverse fault, was an E-W transfer fault system in a N-S system of normal faults during Mesozoic rifting phases; and (2) the recess and salient geometries of the frontal thrust belt across the Chucarima transverse fault are controlled by a lateral change of thickness of lower Cretaceous strata. The lateral changes in structural and stratigraphic patterns across the Chucarima fault, as described here, define the Chucarima transverse zone. Similar relationships between curved geometry of orogenic belts and basin geometry bounded by transverse structures have been documented in other regions (Macedo and Marshak, 1999).

Structure of the Central Cross Section

This section traverses the area where the Guaicaramo fault system has its easternmost advance into the foreland basin, defining a salient geometry of the thrust belt. At this latitude, the Eastern Cordillera reaches its maximum width in a NW-SE direction. This cross section starts at the hanging-wall block of the east-verging Pesca fault, the southern equivalent to the basement-rooted Soapaga fault system to the north (Fig. 1). This cross section passes through the Llanos foothills with no exposures of basement blocks and reaches the Llanos Basin (Fig. 3B). Farther south along the Llanos foothills, the Quetame massif plunges northward at the same latitude where other folds plunge, and the Guaicaramo fault system is displaced to the west to become the Servita fault. The alignment of these elements corresponds to the Sabanalarga transverse zone; structures that strike parallel to this transverse zone show evidence of reactivation (Mora et al., 2006). We interpret this transverse zone as a buried E-W transfer fault system composed of Mesozoic normal faults, as suggested by Sarmiento-Rojas et al. (2006) in this area and farther south in a system named the Nazareth transfer zone.

Although basement rocks are not exposed along the eastern flank of the Eastern Cordillera between the Chucarima and Sabanalarga transverse zones, we interpret basement-rooted faults as the boundaries of structural domains in

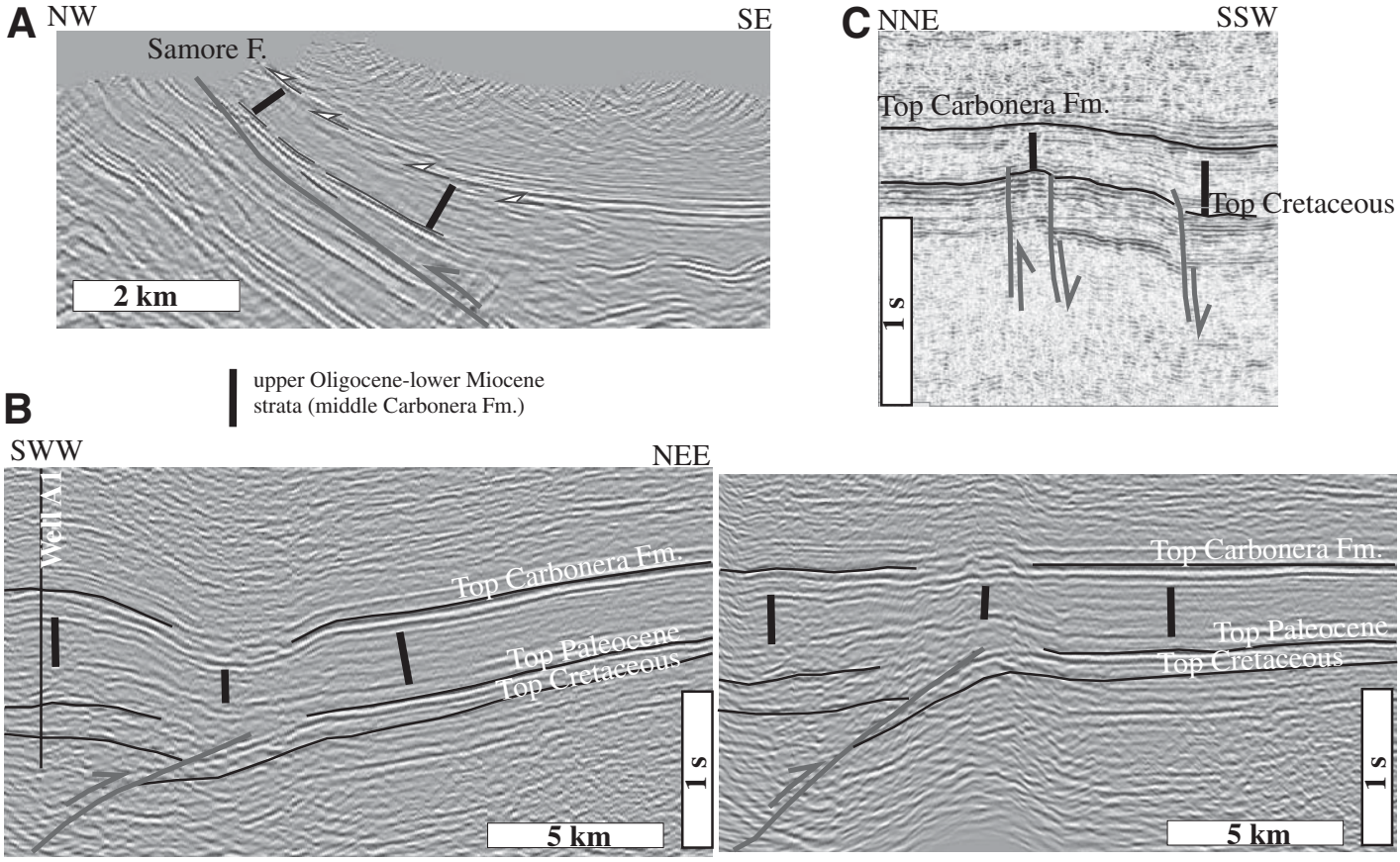

Figure 4. Evidence of faulting during deposition of upper Oligocene–lower Miocene Carbonera strata (thick black line) in the northern cross section (see Fig. 3A for location of seismic lines). From west to east: (A) Depth-migrated seismic line across the western flank of a hanging-wall syncline showing growth-strata patterns; arrows indicate the onlap relation of strata. (B) Left: time-migrated seismic line showing lateral thickness change across an anticline structure in the western Llanos Basin. Right: line flattened to the top of the Carbonera Formation showing the thinning of strata at the axial zone of the anticline. (C) Time-migrated seismic line showing thickening of the Carbonera Formation across extensional structures in the Llanos Basin.

the Eastern Cordillera and Llanos foothills. Pre-Mesozoic metamorphic and sedimentary rocks exposed in the Floresta massif in the axial zone of the Eastern Cordillera and the Quetame massif to the south of the Sabanalarga transverse zone support this assumption. These basement-rooted faults (domains DC1&2, Fig. 3B) are interpreted as reactivated normal faults because of the contrasting stratigraphic thickness variations of Paleozoic-Mesozoic successions between structural blocks (Mora et al., 2006; Kammer and Sanchez, 2006). The Llanos foothills area includes the east-verging Guaicaramo fault system, overturned Neogene beds in the adjacent syncline, and low-angle thrust faults at the leading edge of the deformation front. The Guaicaramo fault system includes a symmetrical syncline in the hanging wall and offsets an asymmetrical overturned anticline-syncline pair (domain DC3). To the east, Ordovician, upper Cretaceous, and Cenozoic strata are involved in east-verging low-angle thrust fault systems (domain DC4; Martinez, 2006). These faults deform the eastern flank of wide and laterally continuous synclines; both frontal faults and synclines form an en echelon array along the eastern boundary of the Llanos foothills. In the Llanos Basin (domain DC5), upper Cretaceous and Cenozoic rocks dip gently westward and overlie Paleozoic and basement crystalline rocks. Basement structures locally offset the sedimentary wedge.

The total shortening estimated for this cross section is 43 km (Fig. 3B). Basement-involved structures transfer displacement at shallow depths into a dominantly east-verging fold-and-thrust belt with décollement surfaces at several levels within Cretaceous and Oligocene rocks (Figs. 2 and 3B). West-verging fault systems in the axial zone of the Eastern Cordillera are interpreted as back thrusts that deform the footwall block of the Pesca fault (domain DC1). The east-verging basement-cored anticline-syncline pair in the Llanos foothills is interpreted as an overturned and displaced fault-propagation fold because: (1) beds in the hanging wall and footwall blocks of the Guaicaramo fault system are overturned and have high-angle dip, and (2) the Guaicaramo fault system displaced overturned beds of the eastern flank of the anticline. Kinematic modeling of similar structures (Narr and Suppe, 1994) indicates that basement-involved structures within the anticline forelimb contribute to the formation of asymmetrical overturned synclines in the front. As the anticline developed, deformation played a more important role in controlling the location and architecture of synorogenic Cenozoic deposition eastward of the Guaicaramo fault system. As shortening increased, the asymmetrical fault-propagation fold broke along the major fault system, and the hanging wall overrode the overturned flank of the asymmetrical syncline. Seismic reflectors of upper Oligocene and Miocene strata do not show growth-strata patterns above the uppermost detachment level (Toro et al., 2004); however, this detachment level cut off structures involving Paleogene strata, suggesting incipient deformation beginning in the Oligocene in the Llanos foothills (Rathke and Coral, 1997; Martinez, 2006). In addition, out-of-sequence reactivation is inferred from offset of fold axes across the east-verging Chameza fault and from the irregular hanging-wall and footwall cutoff patterns of the Guaicaramo fault system.

Two other styles of deformation are interpreted for the Llanos foothills (domain DC4, Fig. 3B). The first style is observed on the western segment, where fold geometry is related to a ramp-flat geometry of the basement-rooted Yopal fault and where there is an upper décollement surface in upper Eocene rocks. The other style is interpreted on the eastern segment, where fold geometry is associated with the propagation of the east-verging Cusiana fault system, which has a décollement surface in Ordovician sedimentary rocks and breaks to the surface along the frontal limb of the syncline. The latter style is complex at depth due to (1) an out-of-sequence west-verging fault system that offset the east-verging fold-and-thrust system (Martinez, 2006), and (2) the subsequent truncation of footwall structures by the east-verging Yopal fault.

MAASTRICHTIAN–PLIOCENE TECTONO-STRATIGRAPHIC SEQUENCES

A tectono-stratigraphic sequence in a foreland basin is a rock unit genetically related to one tectonic loading event, and it may be constrained by the internal architecture of foredeep strata (Flemings and Jordan, 1990) and lateral migration of foreland basin depozones (DeCelles and Giles, 1996). In a nonmarine siliciclastic tropical foreland basin (i.e., the Llanos Basin), a tectono-stratigraphic sequence is bounded at the base by fine-grained strata in the axial foredeep (high tectonic subsidence and low influx of detritus from the forebulge or orogen) and amalgamated sandstones in the distal foredeep (subsidence decreasing toward the forebulge). In the proximal and axial zone of the foredeep, the tectono-stratigraphic sequence consists of muddy sandstones, sandstones, and conglomerates showing an upsection increase of lithic content supplied from the orogen coincident with decreasing accommodation space. If the forebulge is exposed, a correlative unconformity is the equivalent record of foredeep strata. As the paired load (sedimentary and tectonic) and flexural wave advance cratonward, dark-colored mudstones of the axial foredeep migrate cratonward, while deposition of amalgamated sandstones takes place on the former forebulge. If new tectonic loading breaks back within the hinterland or the tectonic loading configuration changes abruptly, the foreland geometry will change, and a new tectono-stratigraphic sequence will be formed.

The Maastrichtian-Pliocene stratigraphic succession can be divided into five tectono-stratigraphic sequences (Figs. 5 and 6), the chronological intervals of which are constrained by palynological data (see methods in Jaramillo et al., 2006a, 2006b). Palynological age determinations have the following resolution: 1–2 m.y. for the Maastrichtian-Paleocene, 5–10 m.y. for the Eocene, 3 m.y. for the Oligocene, and 1–2 m.y. for the early and middle Miocene. In this section, we focus on lateral and vertical changes of lithofacies associations and key sedimentological data for Maastrichtian–middle Miocene tectono-stratigraphic sequences, and we present a brief description of the middle Miocene–Pliocene sequence. Lithostratigraphic units of the Llanos foothills area are indicated in the headers for each tectono-stratigraphic sequence, and equivalent lithostratigraphic units are indicated in Figures 5 and 6.

Tectono-Stratigraphic Sequence One (Upper Maastrichtian to Lower Lower Paleocene; Upper Guadalupe-Guaduas Formations and Equivalent Strata)

A regional shift from marginal to coastal fluvial depositional environments is recorded in this sequence. A brief description of this shift is presented from east to west. In the central Llanos foothills, Guerrero and Sarmiento (1996) reported a 150-m-thick coarsening-upward succession from medium-grained to conglomeratic sandstones with cross-beds and reworked bivalves, oysters, and corals (Fig. 5). Bioturbation is observed both in sandstone and black mudstone beds. These Maastrichtian conglomeratic sandstones have been reported up to 200 km farther north along the Llanos foothills (e.g., Colmenares, 1993; Arango, 1996), and fine-grained interbeds show recovery of pollen and dinoflagellate cysts that indicate a Maastrichtian age (Bayona et al., 2006). In the northern Llanos foothills, fine-grained siliciclastic successions and thin carbonate interbeds dominate (Royero, 2001; Geoestratos-Dunia, 2003). A 30–40-m-thick succession of Maastrichtian carbonaceous mudstones overlies the conglomeratic sandstones (Fig. 5, section TN).

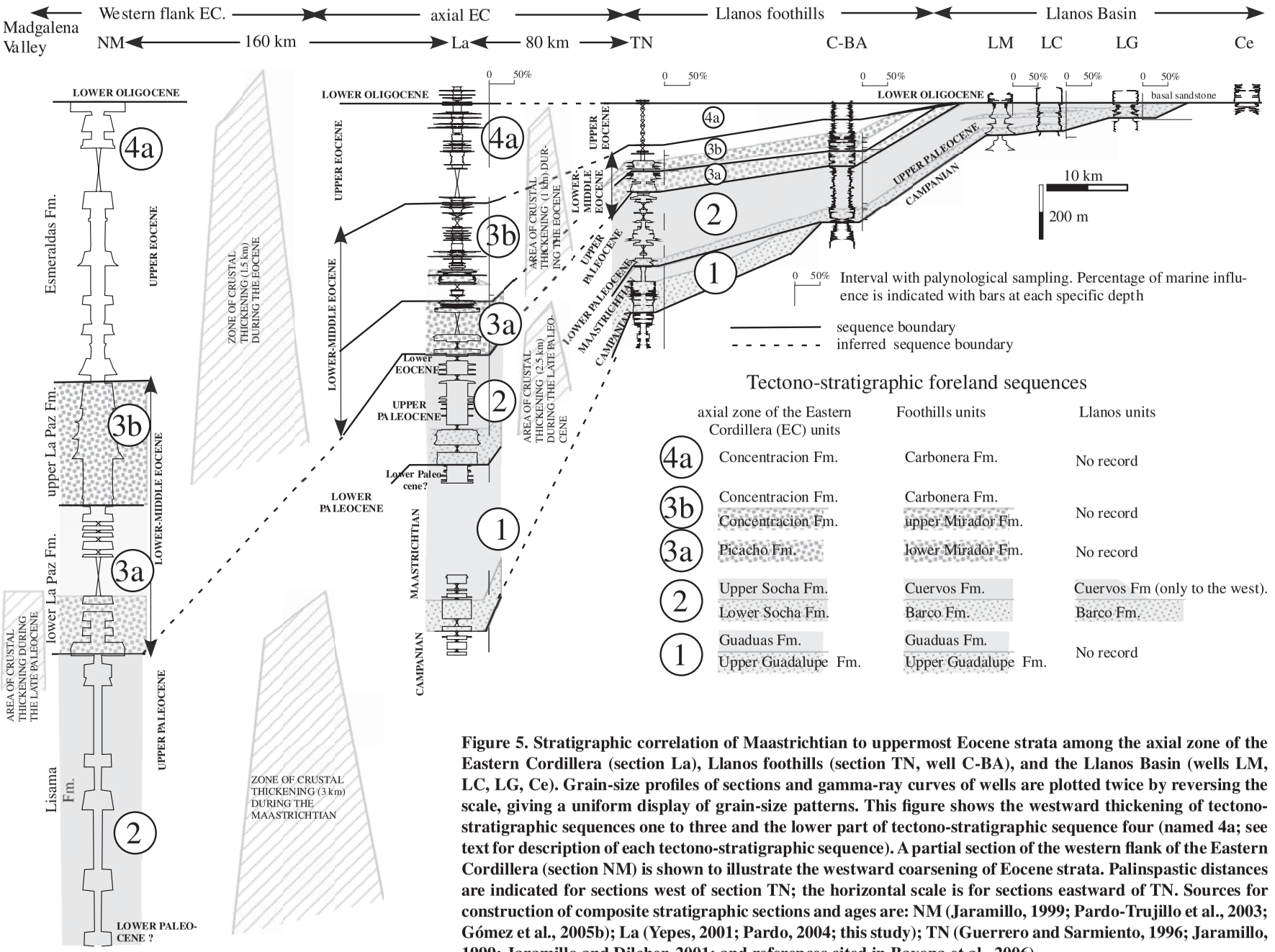

Figure 5. Stratigraphic correlation of Maastrichtian to uppermost Eocene strata among the axial zone of the Eastern Cordillera (section La), Llanos foothills (section TN, well C-BA), and the Llanos Basin (wells LM, LC, LG, Ce). Grain-size profiles of sections and gamma-ray curves of wells are plotted twice by reversing the scale, giving a uniform display of grain-size patterns. This figure shows the westward thickening of tectono-stratigraphic sequences one to three and the lower part of tectono-stratigraphic sequence four (named 4a; see text for description of each tectono-stratigraphic sequence). A partial section of the western flank of the Eastern Cordillera (section NM) is shown to illustrate the westward coarsening of Eocene strata. Palinspastic distances are indicated for sections west of section TN; the horizontal scale is for sections eastward of TN. Sources for construction of composite stratigraphic sections and ages are: NM (Jaramillo, 1999; Pardo-Trujillo et al., 2003; Gómez et al., 2005b); La (Yepes, 2001; Pardo, 2004; this study); TN (Guerrero and Sarmiento, 1996; Jaramillo, 1999; Jaramillo and Dilcher, 2001; and references cited in Bayona et al., 2006).

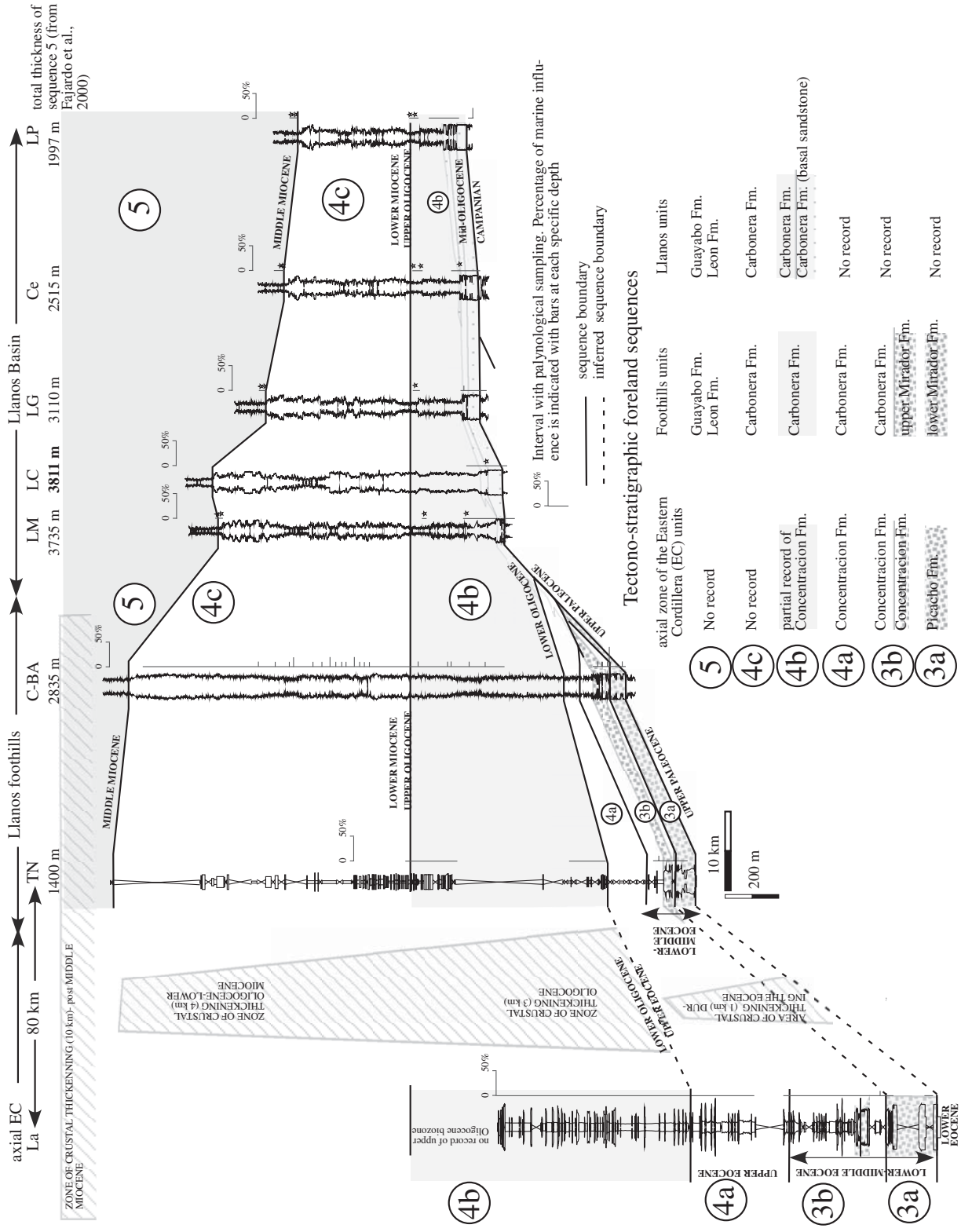

Figure 6. Stratigraphic correlation of Eocene to middle Miocene strata among the axial zone of the Eastern Cordillera (section La), Llanos foothills (section TN, well C-BA), and the Llanos basin (wells LM, LC, LG, Ce, LP). Grain-size profiles of sections and gamma-ray curves of wells are plotted twice by reversing the scale, giving a uniform display of grain-size patterns. This figure illustrates tectono-stratigraphic sequences three and four and the lower part of sequence five. The abrupt thickening of these sequences migrates eastward, reaching the thickest succession of sequence five in well LC (3811 m). Palinspastic distance between sections La and TN is indicated; the horizontal scale is for sections eastward of TN. Sources for construction of composite stratigraphic sections and ages are: La (Pardo, 2004; this study); TN (Jaramillo, 1999; Jaramillo and Dilcher, 2001; and references cited in Bayona et al., 2006).

Along the axial zone of the Eastern Cordillera, strata of this sequence are represented by fine- to medium-grained sandstones with cross-beds and abundant ichnofossils (Perez and Salazar, 1978; Fabre, 1981). These beds are overlain by a unit that consists in the lower half of fine-grained strata with abundant coal seams and in the upper half of laminated mudstones and massive light-colored mudstones (Sarmiento, 1992). The thickness of this unit is variable; there is a 1100 m depocenter near Bogotá, and it thins eastward to less than 450 m and northward to less than 300 m near the Santander massif (Fabre, 1981; Royero, 2001). Maastrichtian–lower Paleocene units in the Magdalena Valley include conglomeratic units derived from the Central Cordillera to the south (Gómez et al., 2003), whereas to the north, carbonate silt and mudstones dominate (Gómez et al., 2005b). Maastrichtian strata are absent in the southern Llanos Basin (Bayona et al., 2006), in the frontal thrust sheets of the central Llanos foothills and Llanos Basin (Cooper et al., 1995), as well as along the frontal thrust sheets of the western flank of the Eastern Cordillera (Bayona et al., 2003).

Tectono-Stratigraphic Sequence Two (Upper Lower Paleocene to Upper Paleocene; Barco-Cuervos Formations and Equivalent Strata)

Biostratigraphic data indicate that fine-grained strata of this tectono-stratigraphic sequence in the axial zone of the Eastern Cordillera correlate with aggradational, fine-to-coarse-grained quartzarenites in the Llanos Basin (Fig. 5). This succession changes upsection from: (1) cross-bedded, fine- to coarse-grained upward-fining quartzarenites (Fig. 7A), locally conglomeratic in Cocuy (Fabre, 1981) and section La (Pardo, 2004) (this unit pinches out west of Bogotá; Hoorn, 1988); to (2) interbeds of upward-fining sandstone and mudstone with bidirectional cross-bedded and bioturbated heterolithic laminated sandstone; (3) locally bioturbated dark-gray organic-rich claystone and mudstone with thin coal seams and excellent pollen recovery; and (4) at the top, massive light-colored sandy mudstone with very poor pollen recovery. This uppermost lithology contains isolated sandstones with upward-fining and coarsening grain-size trends with cross-beds, wavy lamination, and ripple cross-lamination (Figs. 7B and 7C). The thickness of this tectono-stratigraphic sequence decreases eastward and northward: in the Bogotá area, it varies from 0.9 to 1.2 km (Hoorn, 1988), in sections La-Cocuy-Va (western end of cross sections in Fig. 1), it ranges from 0.4 to 0.8 km (Fabre, 1981; Pardo, 2004; Geoestratos-Dunia, 2003), in the Llanos foothills, it ranges between 0.6 and 0.2 km, and in the Llanos Basin, it ranges from 0 to 0.2 km (Figs. 1 and 5).

The vertical arrangement of lithofacies and palynofacies has been interpreted as a product of deposition, from base to top, in fluvial, fluvial-estuarine, and coastal-plain systems. Sandstones indicate fluvial influence in the axial zone of the Eastern Cordillera (Pardo, 2004), whereas they are more tidally influenced in the Llanos foothills (Cazier et al., 1995; Reyes, 1996). The fine-grained strata accumulated in floodplains with increasing estuarine influence toward the Llanos foothills. The change from excellent to poor pollen recovery in fine-grained units suggests that deposition of upper strata took place above the water table (Pardo, 2004). Equivalent strata in the Magdalena Valley consist of 1.2-km-thick organic-rich mudstone interbedded with ripple-laminated and cross-bedded lithic sandstone that accumulated in fluvial-deltaic plain environments (Gómez et al., 2005b; section NM in Fig. 5).

Tectono-Stratigraphic Sequence Three (Lower to Middle Eocene; Mirador–Basal Carbonera Formations and Equivalent Strata)

Lithological units of this age are reported only west of the Llanos foothills and consist of two intervals. The lower interval (named 3a in Fig. 5) rests in abrupt contact with strata of sequence two (Fig. 7D) and includes fine- to medium-grained and locally conglomeratic quartzarenites beds that internally are massive, cross-bedded, and wavy-laminated to the top (Fig. 7E). The upper interval (named 3b in Fig. 5) has upward-fining successions and coal interbeds in the northern Llanos foothills (Reyes, 2004), whereas in the central Llanos foothills, sandstones show a diverse ichnofacies association (*Ophiomorpha*, *Thalassinoides*, *Psilonichnus*, and *Diplocraterion*; Pulham et al., 1997), couplets in foreset laminations, and wavy and flaser lamination in upper mudstone interbeds (Parra et al., 2005). Dark-colored mudstones with thin coal seams rest conformably on the bioturbated sandstones (Jaramillo, 1999; Jaramillo and Dilcher, 2001). These two intervals are separated by light-gray massive sandy mudstone and locally laminated, organic mudstone with plant remains (Fig. 5); this level is characterized by moderate abundance of marine indicators, including foraminiferal test lining and several dinoflagellate cysts, such as *Polysphaeridium subtile*, *Achomosphaera* sp., *Spiniferites* sp. *Cordosphaeridium inodes*, and *Nematosphaeropsis* (Jaramillo and Dilcher, 2001).

The lower and upper intervals are also present in the axial zone of the Eastern Cordillera (section La in Fig. 5). The lower interval (3a in Fig. 5) includes cross-bedded, medium- to coarse-grained sandstone and conglomeratic sandstone, which changes upsection to interbeds of tabular-bedded fine-grained sandstone and discontinuous mudstone interbeds (Céspedes and Peña, 1995; Pardo, 2004). The upper interval (3b in Fig. 5) includes laminated gray mudstone with some interbeds of sandstone and oolithic sandstone (Reyes and Valentino, 1976). The thickness of this sequence in section La is twice as thick as in the Llanos foothills (Fig. 5). Farther west in the Magdalena Valley, coeval lower and middle Eocene strata are as much as 1 km thick and consist of conglomeratic sandstone, multistoried cross-bedded sandstone and mudstone (Restrepo-Pace et al., 2004; Pardo-Trujillo et al., 2003; Gómez et al., 2005b).

Sandstones of the lower interval have been interpreted as amalgamated fluvial channels, whereas sandstones of the upper interval record a stronger influence of brackish and marine conditions. In the central Llanos foothills, these beds accumulated in mouth-bar and coastal-plain settings (Cazier et al., 1995; Fajardo, 1995; Warren and Pulham, 2001), whereas in the northern Llanos foothills and axial zone of the Eastern Cordillera, they accumulated in a more continental setting (Fajardo-Peña, 1998; Reyes, 2004).

Tectono-Stratigraphic Sequence Four (Upper Eocene to Middle Miocene; Carbonera Formation and Equivalent Strata)

Lowermost strata of tectono-stratigraphic sequence four vary laterally from fine-grained deposits in the axial zone of the Eastern Cordillera, Llanos foothills, and northern Llanos Basin to amalgamated sandstones in the central Llanos Basin (intervals 4a and 4b in Fig. 6). Fine-grained strata include laminated dark-gray mudstone with thin seams of coal and bioturbated fine-grained sandstone (Mora and Parra, 2004) in the Llanos foothills and dark-colored mudstone resting upon the unconformity in the northern Llanos Basin. Amalgamated to upward-fining successions of fine- to coarse-grained sandstone and conglomeratic sandstone show an onlap relation with the unconformity in the central and southern Llanos Basin (Bayona et al., 2006).

Strata overlying these lowermost beds have a more uniform upward-coarsening grain-size trend in the axial Eastern Cordillera, Llanos foothills, and Llanos Basin (interval 4b in Fig. 6). An upward-coarsening succession includes laminated mudstone with mollusks (Parra et al., 2005) and marine- to brackish-water indicators at the base (Fig. 6), which grade to tabular

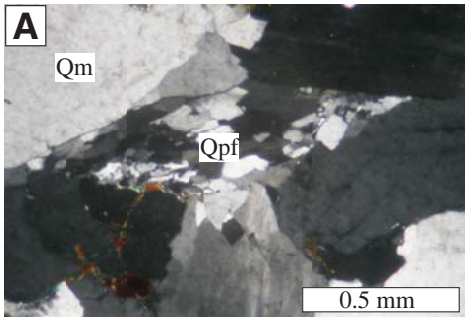

Qm— monocrystalline quartz
Qp— polycrystalline quartz
Qpf— foliated polycrystalline quartz
Qc— cryptocrystalline quartz (chert)
Lm— metamorphic lithic fragment
Pgl— plagioclase fragment

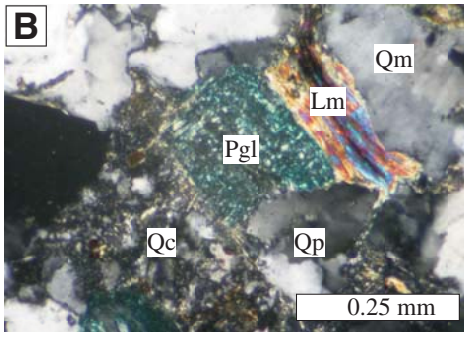

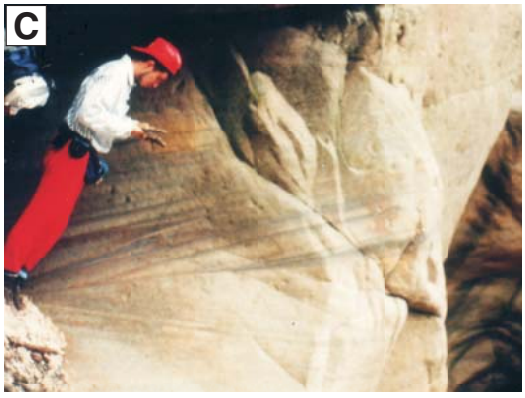

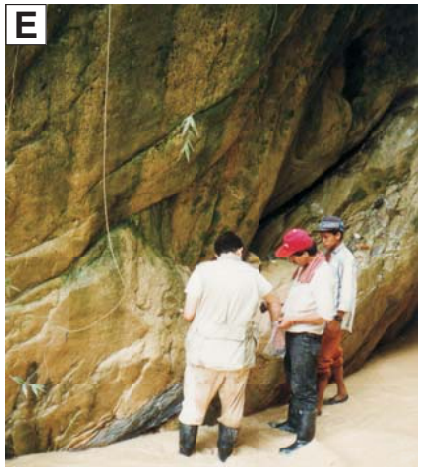

Figure 7. (A–B) Abrupt change in sandstone composition within tectono-stratigraphic sequence two in Cocuy area (northern area, Fig. 1). (A) Quartzarenite of the lower upper Paleocene Barco Formation. (B) Sublitharenite of the middle upper Paleocene Cuervos Formation. (C–G) Outcrops around section TN (central cross section). (C) Sets of planar cross-bedding in the upper Paleocene Cuervos Formation; lithic fragments are concentrated along the cross-beds. (D) Topographic contrast at the contact between Cuervos (valley) and Mirador Formations (scarp). (E) Amalgamated channels of the Mirador Formation with thin mudstones interbeds (tectono-stratigraphic sequence three). (F) Coarsening-upward succession at the top of the Carbonera Formation (tectono-stratigraphic sequence four), which is coeval with deposition of shale of the Leon Formation in the Llanos Basin (Parra et al., 2005). (G) Mottled reddish mudstones (paleosols) interbedded with sandstones of the Guayabo Formation (tectono-stratigraphic sequence five).

and wavy laminated, locally bioturbated, fine-grained sandstone. In the central Llanos foothills, these successions include coal seams, feldspar-bearing fine-grained muddy sandstone, and locally conglomeratic cross-bedded sandstone (Parra et al., 2005). Upward-coarsening successions dominate in the Llanos foothills, with some incursions of brackish waters (Figs. 6 and 7F), whereas in the Llanos Basin, upward-fining trends are more common toward the top of this sequence (interval 4c in Fig. 6).

The northward and eastward lateral change of depositional patterns supports an interpretation of an eastward-prograding fluvial-deltaic plain developing into a coastal plain (or savannas) and a coeval lacustrine-lagoonal depositional system to the east (Mora and Parra, 2004; Bayona et al., 2006). In the Llanos Basin, the abrupt change in lithological associations of the lowermost beds has been interpreted as a change from channel-fill processes in fluvial systems to transgressive tidal flats and delta bays with minor brackish-water influence changing upsection to a lacustrine environment (Fajardo et al., 2000). The lacustrine system interfingers on the east with a fluvial system draining the Guyana craton and on the west with prograding deltaic systems. Strata at the top of this sequence record fluvial systems across the Llanos Basin (interval 4c in Fig. 6).

Tectono-Stratigraphic Sequence Five (Middle Miocene to Pliocene; Leon and Guayabo Formations)

The uppermost tectono-stratigraphic sequence consists of two lithological units that are recorded partly in the Llanos foothills and occupy most of the Llanos Basin. The lower unit consists of dark-colored laminated mudstone and shale with an isolated record of mollusks and foraminifera (Bayona et al., 2006; Fig. 6). This unit is slightly younger westward, as shown in the southern Llanos Basin (Bayona et al., 2006), and sandstone interbeds increase northward and westward (Cooper et al., 1995; Fajardo et al., 2000). In the Llanos foothills, this unit consists of wavy laminated, bioturbated, and varicolored mudstone interbedded with tabular-bedded, bioturbated quartzarenite (Geoestratos-Dunia, 2003). The upper unit includes varicolored mudstone, lithic-bearing sandstone, and conglomerate, and the coarser lithologies dominate toward the top (Fig. 7G). The maximum recorded thickness is in the Llanos Basin (in well LC in Fig. 6), and not in the Llanos foothills, as in sequence four. The stratigraphic position of the upper unit indicates a post–middle Miocene age.

These units represent the onset of coarse-grained fluvial systems covering the Llanos foothills and Llanos Basin. The lower unit documents westward flooding of a broad fluvial-deltaic system followed by regional onset and establishment of lacustrine-lagoonal environments (Hoorn, 1994), but with less brackish-water influence than that reported in Eocene strata. In contrast, the upper unit represents the eastward advance of a coarse clastic wedge accumulated in fluvial and alluvial-fan systems.

PROVENANCE AND PALEOCURRENTS

Sandstone composition in a tropical nonmarine foreland basin, such as the Llanos Basin and restored eastern flank of the Eastern Cordillera since the latest Cretaceous, is controlled mainly by chemical weathering and composition of source areas. Late Paleocene paleoclimate conditions (mean annual temperature = 23.8 ± 2.1 ºC, mean annual precipitation = 3.4 m/yr; Herrera, 2004) and number of morphospecies (Jaramillo et al., 2006a) were similar to the present tropical rain forest. Changes in composition of modern fluvial sands in the Venezuela Llanos Basin indicate that unstable lithic fragments are not preserved more than 200 km from the Andes of Merida (the source area), and sands with more than 25% of lithic fragments lie mostly within 100 km of the Andes (Johnsson et al., 1991). We consider these distances to be the maximum possible for source areas for the Paleocene basin, bearing in mind that tropical climatic conditions controlled chemical weathering processes in source and basin areas.

Integration of paleocurrent indicators and sandstone composition from Paleogene rocks in the axial zone of the Eastern Cordillera, Llanos foothills, and Llanos Basin indicates a shift in provenance since the Paleocene (Fig. 8; see Data Repository for a complete list of references and evaluation of data[1]). Maastrichtian to lower Paleocene sandstones of tectono-stratigraphic sequence one contain predominantly quartz fragments and minor feldspars (Fig. 8A) in the Llanos Basin, indicating sediment supply from the Guyana craton. Supply of detritus from the craton is additionally supported by the regional westward migration of the Maastrichtian clastic wedge (Diaz, 1994). In the Bogotá region, sandstone of the upper Guaduas Formation (lower Paleocene) contains unstable siltstone, mudstone (10%), and chert (7%) grains, along with phyllite and trace amounts of feldspar grains, suggesting uplift of nearby blocks (Sarmiento, 1992; Torres, 2003).

[1]GSA Data Repository item 2008078, references and evaluation of petrographic and provenance data, is available at www.geosociety.org/pubs/ft2008.htm. Requests may also be sent to editing@geosociety.org.

Sandstones of sublitharenite and litharenite composition in tectono-stratigraphic sequence two contain polycrystalline quartz and unstable lithic fragments (Fig. 7B), which constitute up to 33% of the framework grains, and some feldspars. Reported lithic grain types include siltstone, chert, gneiss, schist, phyllite and igneous rock fragments. In addition, paleocurrent data indicate a shift to northward directions and an increasing variability of paleocurrent directions at the end of the Paleocene (Figs. 8B and 8C). Provenance and paleocurrent data suggest exposure of basement rocks, such as the Floresta and Santander massifs (Vasquez, 1983; Mesa, 1997), that controlled drainage patterns within the axial zone of the Eastern Cordillera during deposition of tectono-stratigraphic sequence two.

The abrupt change from upper Paleocene litharenites (tectono-stratigraphic sequence two) to lower-middle Eocene quartzarenites and sublitharenites (tectono-stratigraphic sequence three) with feldspars in the clay fraction (Benavides, 2004) coincides with a change in stacking pattern of sandstone beds from isolated channel beds within mudstone at the top of tectono-stratigraphic sequence two to multistoried channel beds in tectono-stratigraphic sequence three (Fig. 5). Paleocurrent data indicate a high dispersion pattern, as would be expected in mature (>10 m.y.) fluvial systems located in areas of slow subsidence. Supply of detritus from nearby uplifted blocks is supported by the presence of Cretaceous foraminifera fragments in the matrix of conglomerates (Céspedes and Peña, 1995) and lithic clasts composed of chert, claystone, siltstone, gneiss, schist, and igneous rock fragments (Mesa, 1997, 2004).

The dominance of quartzose sandstones persists in tectono-stratigraphic sequence four. However, the presence of sublitharenite and subarkose, as well as conglomerate beds containing clasts of chert and Cretaceous fossiliferous limestones, documents the preservation of unstable lithic fragments supplied from uplifted blocks within the Eastern Cordillera.

The dominance of quartzose sandstone composition in Paleogene sandstones in the Llanos Basin suggests that the continuing supply of detritus from the Guyana craton was mixed with chemically stable fragments derived from the Eastern Cordillera. However, this pre-Miocene pattern in the Llanos Basin contrasts with sublitharenites and litharenites in tectono-stratigraphic sequence five (Moreno and Velasquez, 1993), which were derived from the Eastern Cordillera. Palynological samples from fine-grained strata of tectono-stratigraphic sequence five contain pollen, as well as dinoflagellate and foraminifera fragments, of Paleocene and older age (Milton Rueda and Vladimir Torres, 2006,

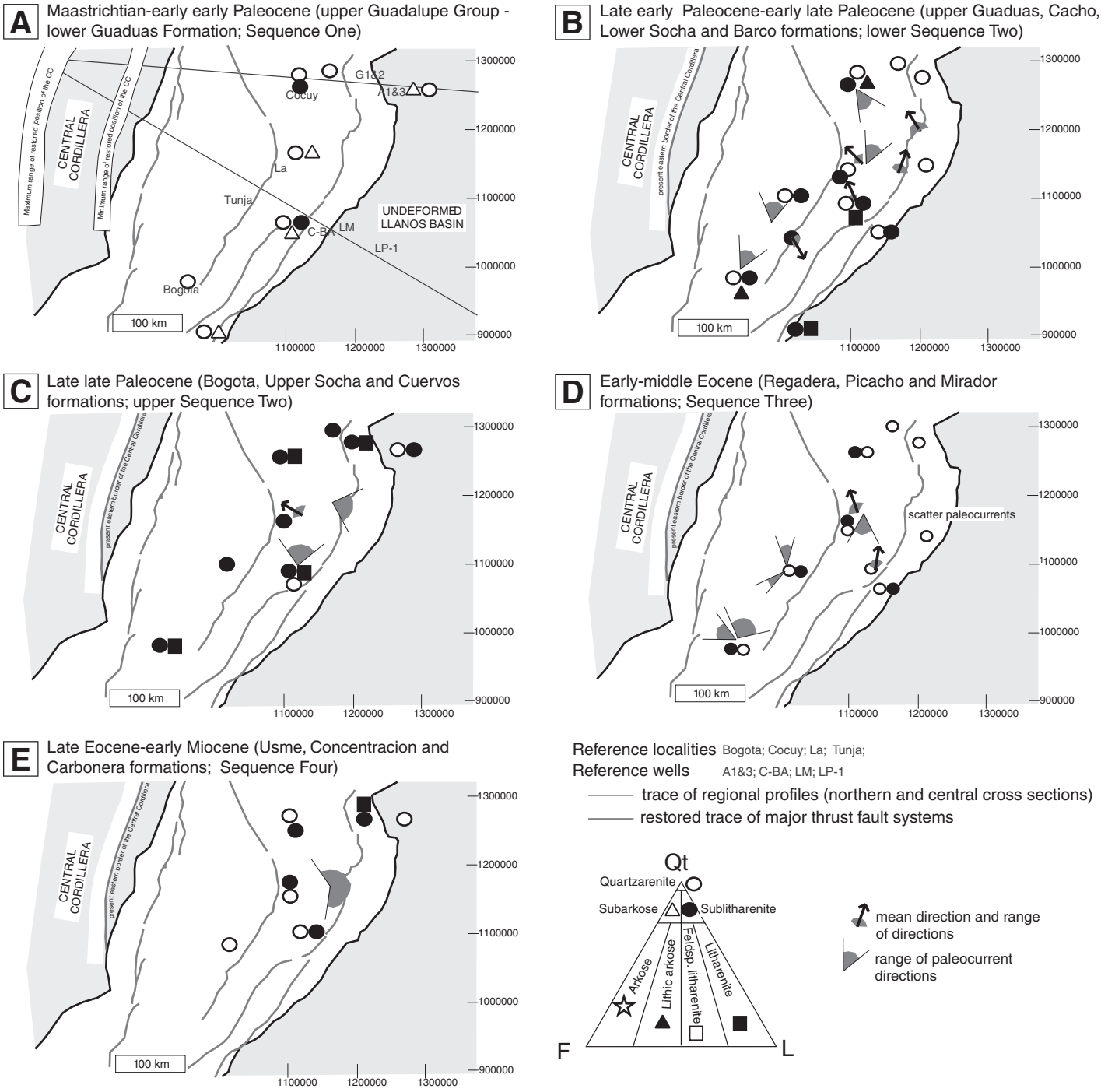

Figure 8. Paleogene palinspastic maps of the inverted Eastern Cordillera (EC) and adjacent Llanos Basin (see details in Fig. 10) showing changes in sandstone composition and paleocurrents for tectono-stratigraphic sequences one to four (see Data Repository for complete list of references [see text footnote 1]). (A) Palinspastic distance between Central Cordillera (CC) and Llanos foothills ranges from 335 to 355 km (Colleta et al., 1990; Cooper et al., 1995; Taboada et al., 2000) to 440–460 km (Dengo and Covey, 1993; Roeder and Chamberlain, 1995); the shorter distance is shown for parts B to E. Source areas in the restored Eastern Cordillera need to be considered to explain the presence of litharenites. See discussion in the text about provenance and paleocurrent data for evidence that supports the interpretation of block uplifts within the Eastern Cordillera.

personal commun.) and document unroofing of the Eastern Cordillera.

ONE-DIMENSIONAL BACKSTRIPPING AND TWO-DIMENSIONAL FLEXURAL SUBSIDENCE ANALYSIS

A comparison of one-dimensional (1D) tectonic subsidence profiles from sections in the axial Eastern Cordillera, Llanos foothills, and Llanos Basin guided selection of time intervals of comparable tectonic subsidence signatures (Fig. 9). Additionally, 1D backstripping techniques were used to decompact the measured stratigraphic thickness of each section, following the methods and assumptions specified in Watts and Ryan (1976) and Allen and Allen (1992). The Late Cretaceous–Cenozoic first-order sea-level curve of Haq et al. (1987) was used for eustasy correction of 1D tectonic subsidence.

Two-dimensional (2D) backstripping of the two cross sections was carried out following the procedures detailed in Watts (2001) to better quantify the subsidence history of the Llanos foothills and Llanos Basin. In order to properly represent the original basin geometry, the positions of each section were plotted in the Paleogene palinspastic map of Sarmiento-Rojas (2001; Fig. 10), which depicts shortening estimates for the eastern flank of the Eastern Cordillera that agree with restorations of our two balanced cross sections. This palinspastic map constrains (1) the most probable position of tectonic loads (areas with no Cenozoic record), (2) areas with growth strata, and (3) areas with intra-Cenozoic angular unconformities. Next, the minimum and maximum 2D basin depths were defined for each time interval using the compacted and decompacted thickness, respectively, of each section or well. The effect of flexural subsidence due to sediment loading was calculated after basin geometry was defined. The latter exercise permitted calculation of the "observed minimum" and "observed maximum" tectonic flexural subsidence of the basin for each time interval. In this study, the numerical implementation of Bodine (1981), which allows plates of laterally variable elastic thickness to be considered, was applied to model the Llanos foreland basin.

Results of One-Dimensional Backstripping

Breaks between periods of constant subsidence rate allow the discrimination of three subsidence events in the Llanos foothills and Llanos foreland basin (Fig. 9); these closely follow the five tectono-stratigraphic sequences defined previously. The first subsidence event is related to increasing subsidence rates in tectono-stratigraphic sequences one and two, the second corresponds to the time interval of tectono-stratigraphic sequence three, and the last regime shows an abrupt increase in subsidence rates in tectono-stratigraphic sequences four and five. The ages of the breaks in the slope of the curve do not overlap for all sections, suggesting that the onset of each event that caused the increase of tectonic subsidence differed across sections in the study area. However, minor differences in the age of those breaks may be due to lack of resolution of biostratigraphic determinations (see bar error for different intervals in Fig. 9).

We interpret all the breaks in the slope of the tectonic subsidence curve as a result of flexural subsidence related to tectonic and sedimentary loading. Significant differences in the ages of the inflection points between the northern and central cross sections may record diachronous along-strike tectonic loading. The age differences of inflection points on curves for the axial zone of the Eastern Cordillera and the Llanos Basin may represent a flexural response of the lithosphere to foreland-directed migration of tectonic loads.

Results of Two-Dimensional Flexural Backstripping

In this study, we tested two hypotheses of foreland evolution for an 800-km-wide plate. Our first model used a spatially continuous foreland basin with a laterally constant plate flexural rigidity (*Te*) for late Maastrichtian, early Paleocene, and late Paleocene time. Our second model considered uplifts of blocks that separated the foreland basin into two main depocenters, the Magdalena and Llanos Basins, on a plate of laterally variable flexural rigidity (*Te*). We used data from the Magdalena Valley presented in Pardo-Trujillo et al. (2003) and Gómez et al. (2005a) for section NM, and from Restrepo-Pace et al. (2004) for section RM. Geodynamic modeling of these profiles was extended to include the restored position of the axial Central Cordillera and wells in the distal Llanos Basin (Fig. 10). We focused on the area between the axial zone of the Eastern Cordillera and Llanos Basin because the uncertainty of palinspastic restoration increases as we move westward from the axial zone of the Eastern Cordillera to the Magdalena Valley and Central Cordillera (Figs. 1C and 8A).

Model 1: One Basin and Uniform Elastic Thickness

In this hypothesis, the Maastrichtian-Paleocene foreland basin was a flexural response of the lithosphere to loading of the Central Cordillera. The purpose of flexural modeling was to test whether flexure of the lithosphere resulting from the weight of the Central Cordillera could reproduce the geometry of the Maastrichtian-Paleocene foreland as far east as the Llanos Basin. Gómez et al. (2005a) were able to obtain a reasonable fit between the observed and the calculated basin geometry for the Colombian foreland basin using an infinite plate model, a discrete load configuration, and a horizontal density contrast between tectonic loads and adjacent sediment fill. All model runs reported by Gómez et al. (2005a) were performed on a 35 km *Te* plate using a thermochronologically constrained history of uplift for the Central Cordillera and western flank of the Eastern Cordillera. We used a tectonic load configuration similar to the one proposed by Gómez et al. (2005a), but the width of our basin was 40 km narrower (see Figs. 1C and 8A). Our model only considered sections/wells close to the cross sections in order to avoid important changes of thickness of Cenozoic synorogenic strata across these traverse structures, as reported by Parra et al. (2005) and this study.

Model runs using these configurations were not able to match the "observed" (i.e., reconstructed) flexural tectonic subsidence profile (Fig. 11). One cause of the discrepancy between our results and those of Gómez et al. (2005a) is the restored width of the Eastern Cordillera. Because the basin geometry of Gómez et al. (2005a) is 40 km wider than ours, the additional sedimentary load, 40 km wide and ~1.5 km thick to the west of the axial zone of the Eastern Cordillera, contributed to flexural subsidence in the Llanos Basin. Because we used a narrower restored basin, both tectonic and sedimentary loading within the restored Eastern Cordillera were required to match the flexural tectonic subsidence in the Llanos Basin (see next section).

Model 2: Interrupted Foreland Basin and Variable Elastic Thickness

The other hypothesis tested in this study was a foreland basin interrupted by tectonic loads in the middle of the basin, which developed on a lithosphere of laterally variable *Te*. The flexural strength of the northern Andean lithosphere is known to vary laterally from low values near the axis of the east Andean topography to high values over the Guyana craton, as supported by two-dimensional flexural models (Ojeda, 2000; Sarmiento-Rojas, 2001), gravity modeling (Stewart and Watts, 1997), and topography/gravity coherence studies (Ojeda and Whitman, 2002).

For each profile, we applied an estimated *Te* configuration that reflected the lateral variability in flexural strength of the lithosphere inherited from the complex Phanerozoic tectonics of

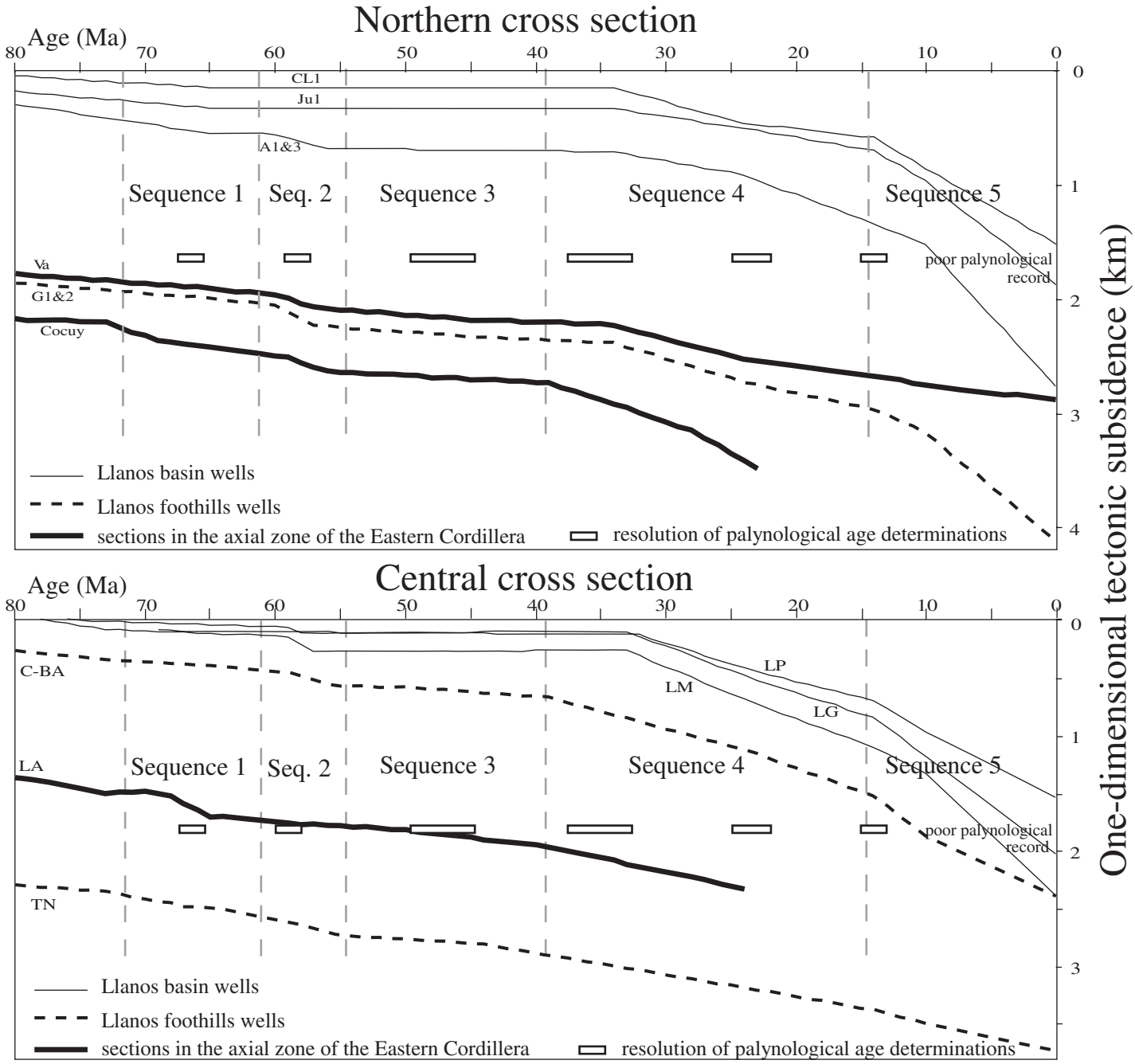

Figure 9. One-dimensional tectonic subsidence curves for selected sections and wells along the northern and central cross sections. Time intervals of the five tectono-stratigraphic sequences are also shown. Cocuy section was modified from Gómez et al. (2005a). Tectono-stratigraphic sequence three records a time interval of very low tectonic subsidence rates, in contrast to Maastrichtian-Paleocene and late Eocene–Pliocene breaks in the slope of the curve. The shape and diachronism of those breaks are interpreted as episodes of flexural subsidence. See Figure 3 for locations of sections and wells.

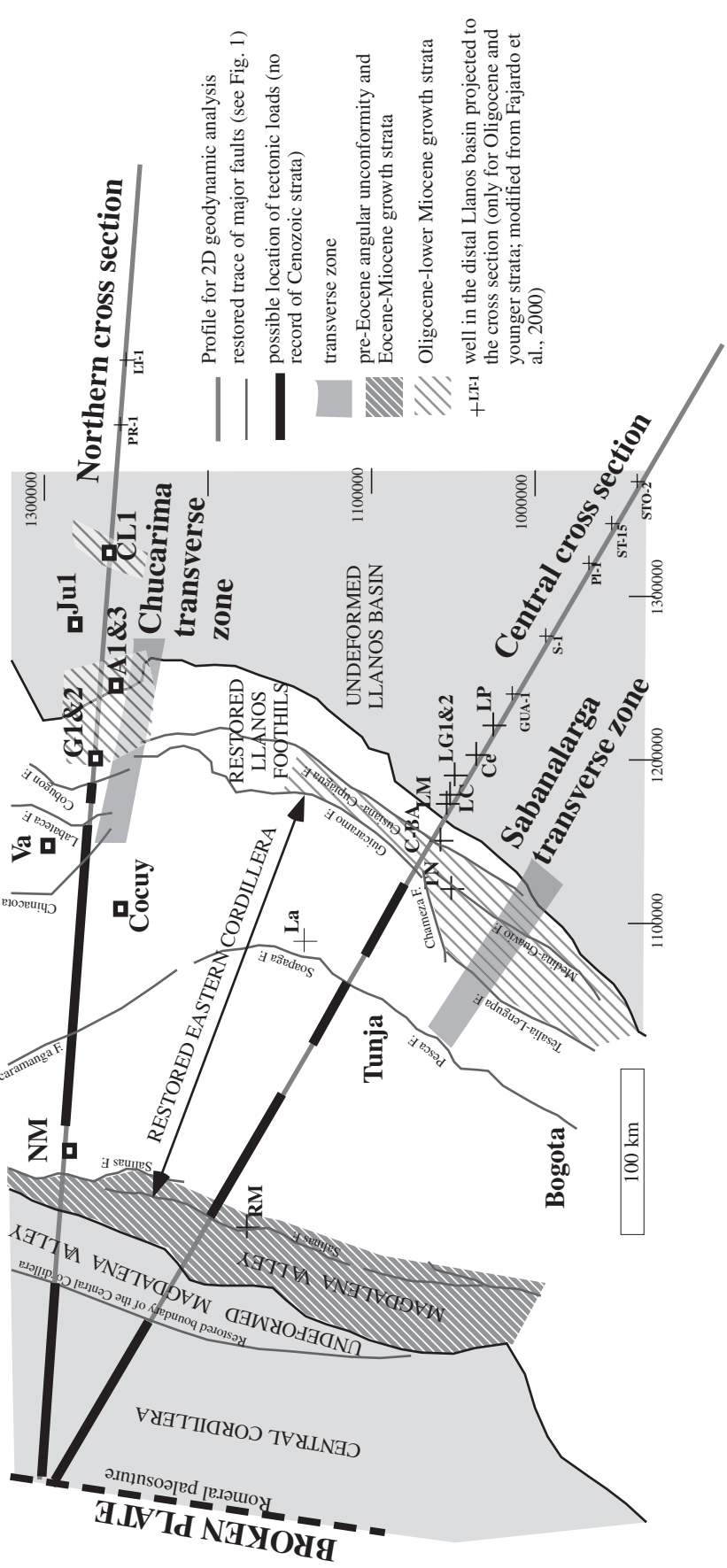

Figure 10. Palinspastic position of sections and wells and trace of the northern and central cross sections (extended to the Central Cordillera) used for two-dimensional (2D) geodynamic modeling, plotted on the palinspastic map of Sarmiento-Rojas (2001). The width of the restored Eastern Cordillera here is similar to the restored width proposed by Colleta et al. (1990), Cooper et al. (1995), and our restored cross sections shown in Figure 3. Present positions of sections/wells are shown in Figure 3, and present traces of major faults are in Figure 1. Growth strata, reported angular unconformities, and areas with no record of Cenozoic strata are also indicated.

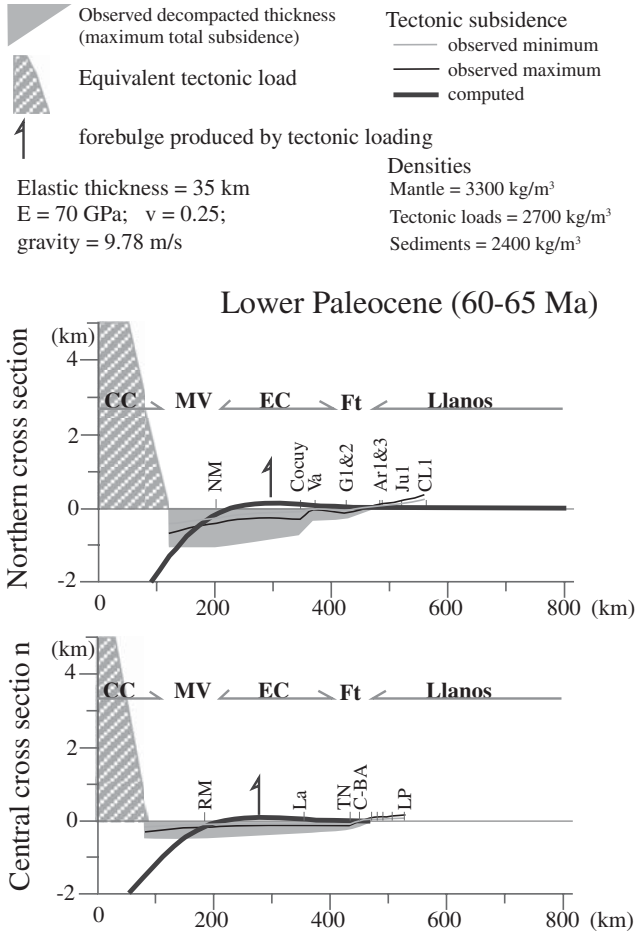

Figure 11. Two-dimensional model for flexural tectonic subsidence using a constant elastic thickness of the lithosphere (35 km), continuous basin geometry for lower Paleocene strata (60–65 Ma), and an 800-km-wide plate with a broken boundary at the restored position of the Romeral paleosuture (see Fig. 1A). Effects of flexural subsidence by sediment loads have been removed to calculate observed flexural tectonic subsidence. CC—Central Cordillera; MV—Magdalena Valley; EC—Eastern Cordillera; Ft—Llanos foothills. See Figures 3 and 10 for actual and restored positions of sections and wells, respectively. This model indicates that tectonic loading is required within the restored Eastern Cordillera in order to match the observed tectonic subsidence in the Llanos Basin as modeled in Figure 12.

Figure 12. Two-dimensional flexural model using variable elastic thickness of the lithosphere (A), interrupted basin geometry since Maastrichtian, and an 800-km-wide plate with a broken boundary at the restored position of the Romeral fault system (see Fig. 1A). Effects of flexural subsidence by sediment loads have been removed to calculate observed flexural tectonic subsidence in two regional cross sections with different geometry of the Guaicaramo fault system (GFS). CC—Central Cordillera; MV—Magdalena Valley; EC—Eastern Cordillera; Ft—Llanos foothills; SM—Santander massif. See Figures 3 and 10 for actual and restored positions of sections and wells, respectively. Note that tectonic loading in the Central Cordillera does not contribute to tectonic subsidence in the Llanos Basin (B and C, see also Fig. 11). For simplicity, we only show tectonic subsidence profiles from the axial zone of the Eastern Cordillera to the Llanos Basin. See text for discussion of models.

northern South America (Fig. 12A). The Guyana craton is relatively thick, thermally relaxed, and rigid (*Te* > 50 km; Stewart and Watts, 1997). We assigned a *Te* in the range of 15–25 km for the lithosphere that underlies the locus of Mesozoic extension (Sarmiento-Rojas et al., 2006). We regarded the lithosphere under the Central Cordillera as tectonically stable and assigned a *Te* value of 55 km for the western end of our profiles. Paleosuture zones, such as the Romeral fault system, are zones of plate rupture (zero flexural strength), or areas of very low flexural rigidity. We considered the palinspastic position of Romeral fault system to be the western edge of our broken plate. An older Paleozoic paleosuture underlying the southern and central Llanos foothills (see Cediel et al., 2003) was represented as a laterally variable *Te* configuration under the central Llanos foothills.

Results of our second set of models were capable of reproducing the tectonic flexural subsidence observed in the Llanos foothills and Llanos Basin, and they honor the paleogeography suggested by stratigraphic and provenance data of our tectono-stratigraphic analyses. Models for the latest Cretaceous–Paleocene are consistent with early uplift of segments of the axial zone of the Eastern Cordillera. Equivalent tectonic loads (i.e., crustal thickening), ranging from 0.5 to 3 km, and synorogenic deposition explain the flexural wavelength and the eastward migration of the flexural wave, as suggested by the Llanos foreland stratigraphy (Figs. 5, 12B, 12C, and 12D). Tectonic loads on the Santander massif in the northern cross section and west of the Pesca fault on the central cross section (west of section La) resulted in development of three distinct depocenters, matching the observed tectonic subsidence. For the late Paleocene, a new foreland-breaking deformation front advanced eastward to create widening accommodation space in the Llanos Basin (Fig. 12D). As the basin stratigraphy and geometry indicate, tectonic loads in the northern cross section (Santander massif) were wider than in the central cross section.

In the early and middle Eocene, the tectonic load–flexural wave pair migrated westward (Fig. 12E), explaining the very low subsidence regime in the study area for tectono-stratigraphic sequence three (Fig. 9). Equivalent tectonic loads on the western flank of the Eastern Cordillera and Magdalena Valley were less than 3 km high on the northern section and less than 2 km high on the central section, with minor loading (<1 km) along the axial zone of the Eastern Cordillera and Llanos foothills. In the late Eocene, loads remained largely unchanged except for minor increases in equivalent tectonic loading.

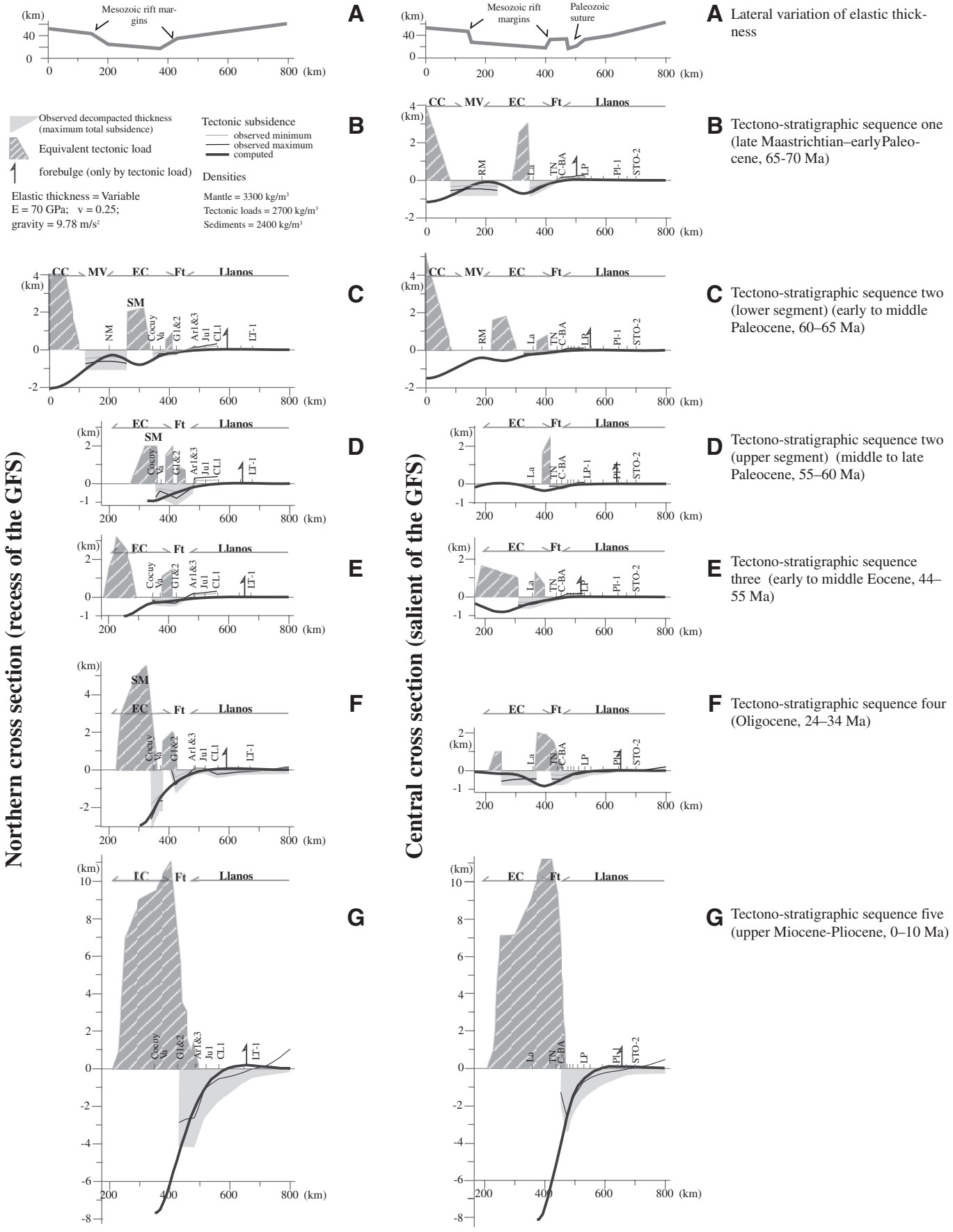

A Lateral variation of elastic thickness

B Tectono-stratigraphic sequence one (late Maastrichtian–early Paleocene, 65-70 Ma)

C Tectono-stratigraphic sequence two (lower segment) (early to middle Paleocene, 60–65 Ma)

D Tectono-stratigraphic sequence two (upper segment) (middle to late Paleocene, 55–60 Ma)

E Tectono-stratigraphic sequence three (early to middle Eocene, 44–55 Ma)

F Tectono-stratigraphic sequence four (Oligocene, 24–34 Ma)

G Tectono-stratigraphic sequence five (upper Miocene-Pliocene, 0–10 Ma)

In Oligocene to early middle Miocene time, tectonic loads consisted of uplift of the Santander massif, the eastern flank of the Eastern Cordillera, and incipient uplifts in the Llanos foothills. The foreland-breaking advance of tectonic loading controlled migration of the flexural wave as recorded by tectono-stratigraphic sequence four (Figs. 6 and 12F). For the Oligocene, equivalent tectonic loads on the northern cross section ranged between 3 and 5 km and were over 150 km wide, whereas for the central cross section, the effective tectonic load, 2 km high and less than 100 km wide, was located in structures between the axial zone of the Eastern Cordillera and central Llanos foothills sections (Fig. 12F). In the early-middle Miocene, tectonic loads advanced eastward toward the present western Llanos Basin and appeared to be the dominant loads (equivalent tectonic loads of 4–6 km) in foreland basin formation. As discussed later, differential loading along the Eastern Cordillera imparted differences in stratal architecture of Oligocene–middle Miocene strata between the central and northern Llanos foothills. For the central cross section, any loads located west of the axial zone of the Eastern Cordillera during this time resulted in subtle subsidence of the Llanos Basin, as demonstrated by Figures 11 and 12C. Therefore, we considered only the effects of tectonic loading to the east of the axial zone of the Eastern Cordillera.

For the middle-late Miocene to Pliocene, the model predicts first a period of considerable decrease of effective tectonic loading followed by a strong uplift of the Andes. Accumulation of the Leon Formation occurred in a basin created by 2 km of equivalent tectonic load west of well Ar1–3 in the northern cross section and west of well C-BA in the central cross section. The load configuration in the late Miocene and Pliocene is consistent with the modern load distribution (Fig. 12G). The coarse-grained Guayabo Formation was deposited in the Llanos Basin as the Eastern Cordillera (equivalent tectonic load of 10–11 km) was emplaced over the adjacent foreland, loaded the lithosphere, and generated a broad flexural sag east of the Cordilleran frontal fault. The uplift of the Eastern Cordillera provided much of the sediment for infill of the sag.

DISCUSSION: LINKAGE BETWEEN THRUSTING AND BASIN EVOLUTION

The integrative approach used in this work predicts the geometry and position of the tectonic loads necessary to produce the observed basin geometry at different time intervals. Our results and published thermochronological-geochronological and paleobotanical data (see references in Evidence of Pre-Neogene Deformation section) provide evidence for at least four shortening events in the axial zone and eastern flank of the Eastern Cordillera prior to the strong post–middle Miocene Andean deformation. These tectonic phases of deformation advanced dominantly eastward from the hinterland (Figs. 13, 14, and 15), but changes in flexural subsidence rates and in the relation between hanging-wall and footwall structures document periods of westward migration of deformation and out-of-sequence reactivation, respectively. In our forward kinematic models for the northern and central cross sections, we translated the positions of tectonic loads into areas where active basement-involved deformation was taking place.

Kinematics of the Northern Cross Section

The earliest phase of foreland development is recorded in Paleocene strata. Flexural deformation may explain: (1) erosion or nondeposition of lower Paleocene rocks in the Llanos Basin and erosion of uppermost Cretaceous rocks farther east, (2) eastward migration of the depositional zero in tectono-stratigraphic sequence two (Barco-Cuervos Formations, Figs. 12C, 12D, and 15B), and (3) increased supply of chemically unstable lithic fragments coincident with increased tectonic subsidence rates (Figs. 8, 11, and 15B). Our geodynamic models indicate that uplifted areas were located mainly at the Santander massif (Figs. 12C, 12D, and 15B), a source area for litharenites in the Cocuy and Va sections less than 100 km away. Although reported zircon fission-track ages in the Santander massif suggest exhumation at this time, the data set of Shagam et al. (1984) needs to be reevaluated with new analyses that consider analytical and conceptual advances of this technique (Andres Mora, 2007, personal commun.). Subsequent, westward migration of tectonic loads to the Magdalena Valley in the early Eocene resulted in deposition of amalgamated sandstones of the thin Mirador Formation and basal shale beds of the Carbonera Formation. (Figs. 12E and 13A).

Field evidence supporting shortening during the Oligocene consists of growth strata in broad synclines in the Llanos foothills and adjacent to a fault-related anticline that formed west of the Llanos Basin (Figs. 4, 12F, 13B, and 15C). Localized normal faulting in the eastern Llanos Basin at this time can be explained as flexural extension at the forebulge, as indicated in our early Oligocene flexural model (Figs. 12F and 15C). Ages of apatite fission tracks in rocks from the Santander massif (Shagam et al., 1984; Toro, 1990) support this interpretation. New zircon and apatite fission-track analyses should be conducted in order to test this hypothesis (Andres Mora, 2007, personal commun.).

Out-of-sequence deformation along the Cobugon and Samore faults in the Llanos foothills is indicated by the truncation of tight anticlines involving Paleogene units by both the east-verging Cobugon fault to the west and the west-verging Samore fault to the east (Figs. 3A, 13C, and 13D). East-verging thrust faults bounding eastern structures of the Llanos foothills involve upper Miocene–Pliocene strata and locally offset Pliocene strata, suggesting post-Pliocene activity for the last phase (Fig. 13D).

Kinematics of the Central Cross Section

The first shortening recorded in this area occurred during latest Cretaceous to late Paleocene time, earlier than in the northern cross section (Figs. 14A, 14B, and 15A). Loads were less than 3 km high and were located west of the Pesca-Soapaga fault system; they subsequently advanced eastward to involve rocks of the eastern flank of the Eastern Cordillera during the late Paleocene (Figs. 12B, 12C, and 15B). These pulses explain the eastward thinning of Maastrichtian-Paleocene sequences one and two, which are bounded at the base by sandstones and conglomerates and, at the top, by fine-grained strata (Fig. 5). Flexural uplift related to the Maastrichtian phase of deformation explains the presence of quartzose sandstone and conglomerate beds in the Llanos foothills (Fig. 15A), which were supplied mainly from uplifted cratonic sources. Flexural extension at the border of the forebulge in the Llanos foothills explains the presence of faults in the Paleocene (65 Ma), as indicated by micas filling vein-wall rocks (Fig. 14A). During the Paleocene, upper Cretaceous strata were eroded in the eastern Llanos foothills and Llanos Basin, and synorogenic deposition of the Barco-Cuervos succession migrated eastward (Figs. 14B and 15B). Unstable lithic fragments indicate that uplifted areas were less than 100 km from the Llanos foothills, Bogotá, and Tunja areas, and those uplifts controlled the northward dispersal of detritus, as indicated by paleocurrent data (Fig. 15B).

During the early and middle Eocene, tectonic loads were located in the Magdalena Valley, as indicated by the angular unconformity underlying Eocene strata and strike-slip deformation. Farther to the east, a period of westward-increasing subsidence took place in the axial zone of the Eastern Cordillera (Figs. 11 and 12E). The amalgamation of fluvial channels of the Mirador Formation indicates low rates of subsidence during this episode of deformation (Figs. 4 and 14C). The presence of lithic fragments and

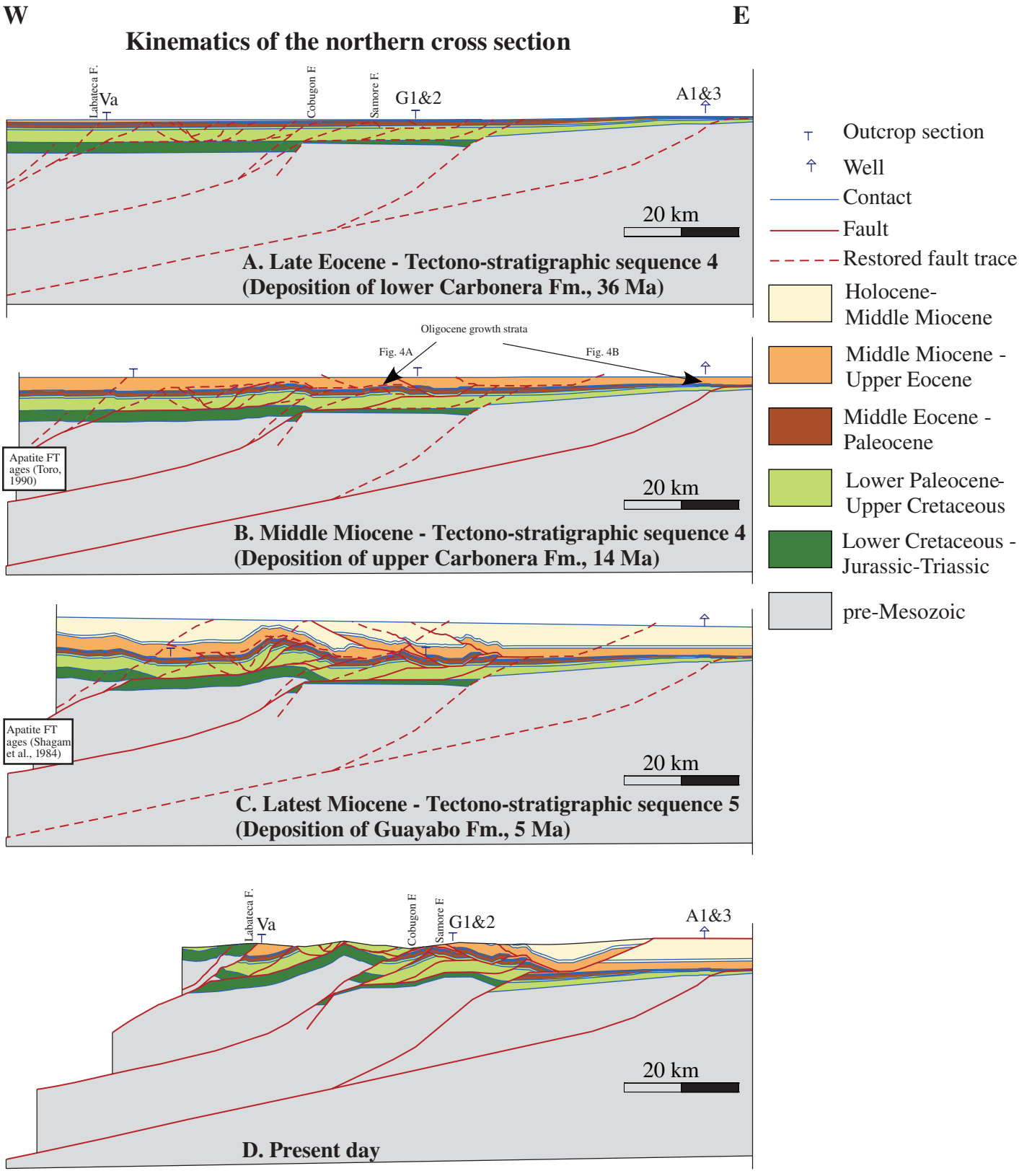

Figure 13. Kinematic forward model for the northern cross section since the middle Eocene. Basin geometry and position of structural activity are constrained by geodynamic modeling, thermochronology, growth structures, and provenance and paleocurrent data. FT—fission track.

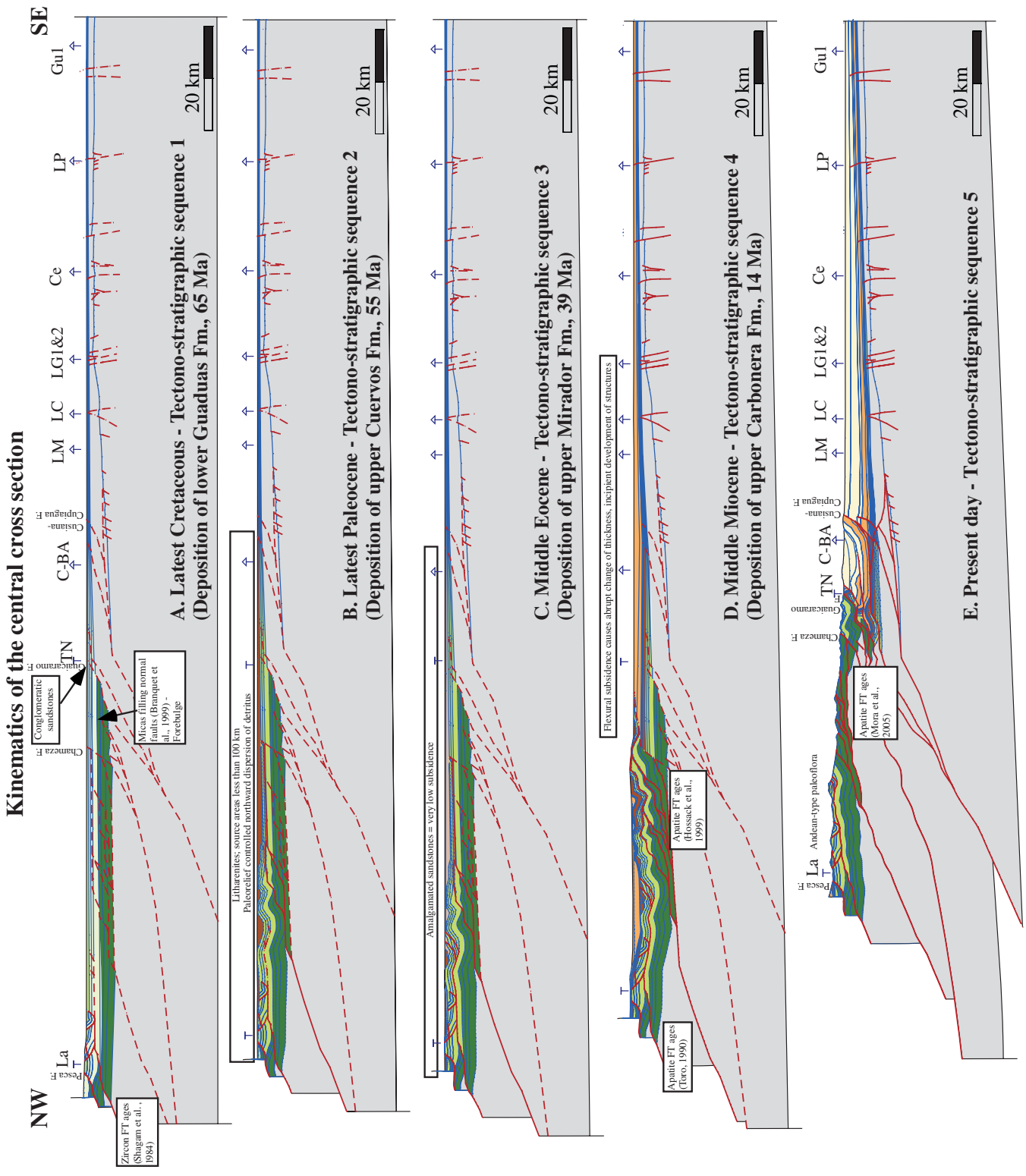

Figure 14. Kinematic forward model for the central cross section since the late Maastrichtian. Basin geometry and position of structural activity are constrained by geodynamic modeling, thermochronology and geochronology data, growth structures, and provenance and paleocurrent data. See explanation of symbols in Figure 13. FT—fission track.

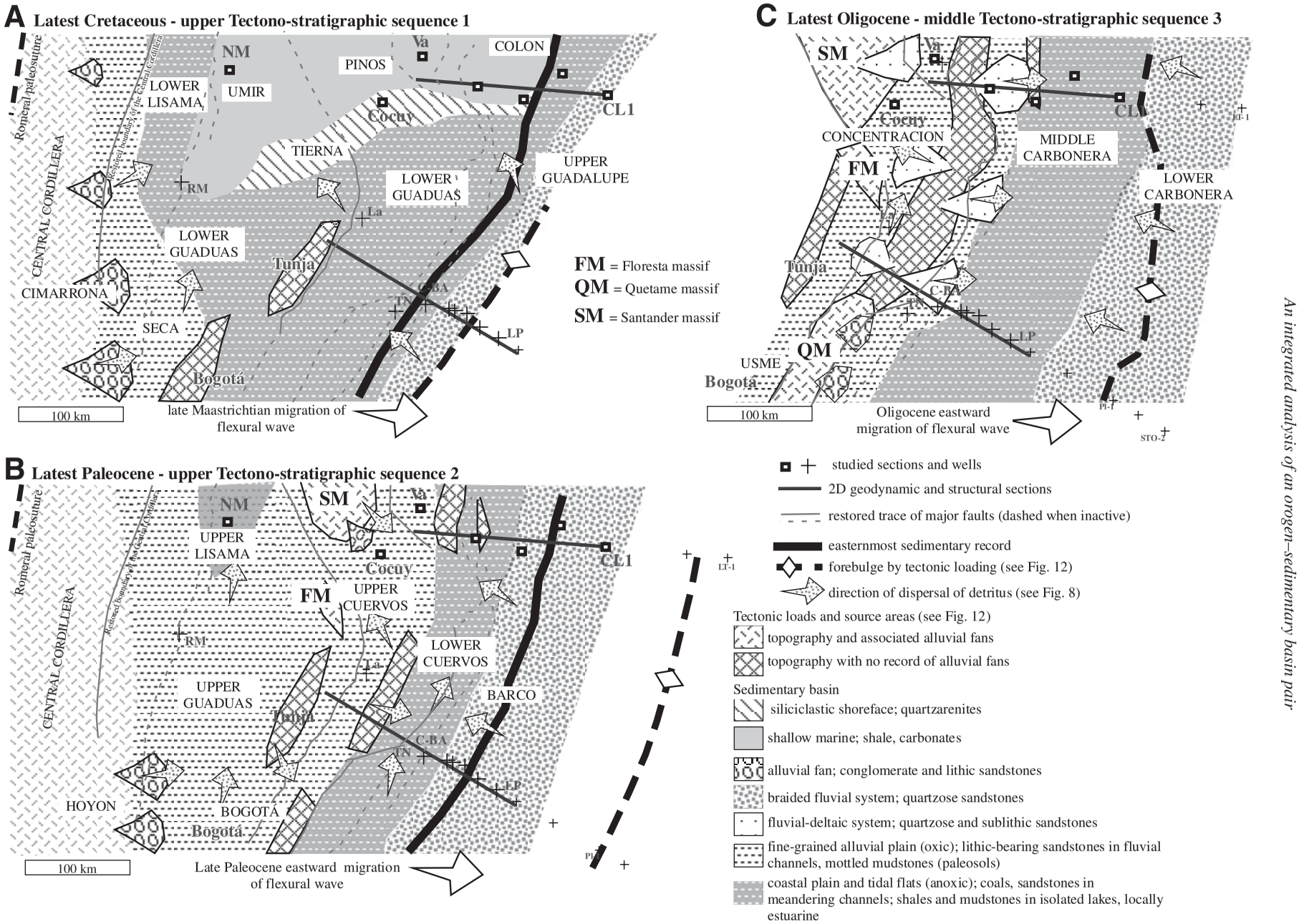

Figure 15. Paleogeographic maps (palinspastic map is from Sarmiento-Rojas, 2001) illustrating three phases of eastward flexural wave migration during (A) late Maastrichtian, (B) late Paleocene, and (C) late Oligocene. See text for discussion. Panels A and B include data for the Magdalena Valley and eastern flank of the Central Cordillera from Diaz (1994) and Gómez et al. (2005a).

fragments of Cretaceous foraminifera in the axial zone of the Eastern Cordillera indicates that minor uplifts continued to supply detritus to the adjacent basin.

Late Eocene to middle Miocene shortening emplaced loads less than 4 km high in the area between the axial zone of the Eastern Cordillera and the eastern Llanos foothills (Figs. 12F, 14D, and 15C). Exhumation of this area, bounded by the Chameza fault to the east, is supported by AFTA data. At this time, a fold-and-thrust belt advanced eastward to the present position of the western Llanos foothills (Fig. 15C), and the salient-recess geometry of the thrust belt began to form. Deposition in the eastern Llanos foothills was mostly accommodated by increasing flexural subsidence toward the Eastern Cordillera (Fig. 12F), as indicated by the abrupt change in thickness of Oligocene and lower Miocene strata, and it was less affected by growth of incipient structures. The dominance of sublitharenite and subarkose supports the interpretation that nearby structures in the eastern Llanos foothills were not exposed to supply detritus to the basin.

Strong basin inversion took place during middle Miocene to Pliocene time and gave rise to today's Eastern Cordillera structural configuration (Figs. 12G and 14E). Equivalent tectonic loads along the eastern flank of the Eastern Cordillera were 10–11 km high, and they advanced eastward to the eastern boundary of the Llanos foothills. The onset of Andean-scale deformation created a regional and nearly simultaneous flooding event that is recorded in most of the sub-Andean foreland basins in the middle Miocene. The rapid uplift and consequent basin filling caused abrupt eastward migration of the forebulge and fluvial-alluvial depositional systems originating from the Eastern Cordillera.

The most active fault during this latter tectonic phase was the Guaicaramo fault system, which allowed exhumation of the Quetame massif and basal Cretaceous strata. It was only at this time that strong surface uplift took place between 6 and 3 Ma, as documented by the change of paleobotanical associations and the generation of an orographic barrier that accelerated deformation on the eastern flank of the Eastern Cordillera. Out-of-sequence deformation along the Guaicaramo fault system was coeval with the different phases of exhumation documented by AFTA data for the Garzon and Quetame massifs.

CONCLUSIONS

The integration of palinspastically restored basin geometry and internal features of syntectonic units (e.g., stratal architecture, sandstone composition, etc.), flexural modeling, and kinematic constraints of the orogenic belt permits identification of phases of deformation in an orogen–foreland basin system. The current configuration of the Eastern Cordillera and adjacent Llanos Basin of Colombia is the result of the polyphase growth of basement-rooted structures and ensuing foreland basin development. Therefore, a comprehensive analysis of the adjacent foreland basin can be used to define the spatial and temporal patterns of deformation of former events in the evolving Eastern Cordillera.

Five episodes of deformation have been documented from analysis of the sedimentary record in the axial zone and eastern flank of the Eastern Cordillera, Llanos foothills, and Llanos Basin. The first three episodes of deformation include shortening during latest Cretaceous to middle Eocene time. During this period, the deformation front first moved eastward from the axial zone to the eastern flank of the Eastern Cordillera (tectono-stratigraphic sequences one and two, Figs. 15A and 15B), and then it shifted to the western flank of the Eastern Cordillera and Magdalena Valley (tectono-stratigraphic sequence three). Flexural deformation induced: (1) erosion of Paleocene–upper Cretaceous strata in the Llanos foothills and Llanos Basin, (2) westward thickening of unconformity-bounded Maastrichtian-Paleocene syntectonic sequences, (3) increased input of lithic fragments in upper Paleocene strata and northward dispersal of detritus, (4) amalgamation of fluvial-to-estuarine channel structures during the early and middle Eocene, (5) change of subsidence rates in the latest Cretaceous and late Paleocene, and (6) slow tectonic subsidence regimes during the early-middle Eocene in the axial Eastern Cordillera and Llanos foothills. These phases of deformation are constrained in the hinterland by: (1) zircon fission-track data from the Santander massif (Shagam et al., 1984); (2) geochronological data from micas filling normal faults associated with flexural extension during the latest Cretaceous (Branquet et al., 1999); and (3) angular unconformities in the Magdalena Valley (Gómez et al., 2003, 2005b). Geodynamic analysis allows us to infer that equivalent tectonic loads for these phases were less that 3 km high, less than 100 km wide, and wider in the northern than in the central part of the study area.

Tectonic loads in the late Eocene–middle Miocene flexural phase were higher than former episodes of deformation, and they were concentrated in the axial zone of the Eastern Cordillera, eastern flank of the Eastern Cordillera, and to a lesser extent in the Llanos foothills. In the northern Llanos foothills, this phase is constrained by the presence of growth strata that bound basement-rooted structures, whereas in the central Llanos foothills, it is mainly constrained by the increasing flexural subsidence toward the Eastern Cordillera and subtle deformation of tectono-stratigraphic sequence four. The fourth tectonic phase was also characterized by eastward reactivation of tectonic loads and generation of the salient-recess geometry of the thrust belt (Fig. 15C). In the hinterland, this phase is identified by published apatite fission tracks (Shagam et al., 1984; Toro, 1990; Hossack et al., 1999). Geodynamic analyses indicate that tectonic loads were 3–6 km high, 50–100 km wide, and wider in the northern than in the central cross section.

The last tectonic episode identified in this study encompassed the width of the entire Eastern Cordillera, involved reactivation of basement structures during middle Miocene to Pliocene time, and ultimately defined the current configuration of major structures that bound the Eastern Cordillera, as well as the flexural geometry of the Llanos Basin. Tectonic loads advanced eastward during at least two periods of out-of-sequence reactivation, as inferred from relations between hanging-wall and footwall structures of the Chameza and Guaicaramo faults in the central cross section, and of the Cobugon and Samore faults in the northern cross section. These phases of deformation are further constrained by rock-exhumation (Van der Wiel, 1991; Mora et al., 2005) and surface-uplift (Hooghiemstra and Van der Hammen, 1998) evidence. However, the lack of biostratigraphic constraints in the associated alluvial and fluvial deposits precludes recognition of individual phases of deformation, similar to those uncovered here for the upper Cretaceous–middle Miocene succession.

The integrative approach used for this research permits identification of the timing of activity on the different structures within the Eastern Cordillera and their effect on the adjacent sedimentary basin. This two-dimensional approach should be considered prior to a three-dimensional analysis of a thrust belt system in order to constrain the effects of a particular phase of deformation on location of source areas, dispersal of synorogenic detritus, distribution of depositional systems, and stratal architecture in the basin. In addition, future thermochronological studies designed to quantify the exhumation of the Eastern Cordillera must encompass the width of the Eastern Cordillera rather than sampling a single range.

ACKNOWLEDGMENTS

This research was supported by the Colombian Petroleum Institute, Ecopetrol S.A., the Smithsonian Paleobiology Endowment Fund, and the Unrestricted Endowments SI Grants. Thanks are due to

the Biostratigraphic Team at the Colombian Petroleum Institute, Nestor Gamba, and Johana Pinilla for their collaboration at different stages of this project. We thank Timothy Lawton for a careful review of the manuscript, which, together with the comments of an anonymous reviewer and Associate Editor James Schmitt, improved the content of this paper. Natasha Atkins reviewed the last revised version of the submitted manuscript to improve the flow of the English. Bayona acknowledges discussions with Elias Gómez concerning foreland evolution of the Magdalena Valley and Llanos Basin, Andres Mora concerning the use of fission-track data and reactivation of Mesozoic structures, and Cornelius Uba, Mauricio Parra, and Brian Horton concerning evolution of Andean foreland systems.

REFERENCES CITED

Allen, P., and Allen, J., 1992, Basin Analysis: Principles and Applications: London, Blackwell Scientific Publications, 451 p.

Arango, F., 1996, Analisis estratigrafico del limite Cretacico Superior-Paleoceno en el bloque colgante de la Falla de Guicaramo en alrededores de Tamara, Casanare: Bogotá, VII Congreso Colombiano de Geologia, Tomo II, p. 516–524.

Bayona, G., Cortés, M., Jaramillo, C., and Llinás, R.D., 2003, The Fusagasugá succession: A record of the complex Latest Cretaceous–pre-Miocene deformation between the Magdalena Valley and Sabana de Bogotá areas, *in* VIII Simposio Bolivariano de Exploración Petrolera en las Cuencas Subandinas: Cartagena, Colombia, Asociación Colombiana de Geólogos y Geofísicos del Petróleo, p. 180–193.

Bayona, G., Reyes-Harker, A., Jaramillo, C., Rueda, M., Aristizabal, J.J., Cortés, M., and Gamba, N., 2006, Distinguishing tectonic versus eustatic flooding surfaces in the Llanos Basin of Colombia, and implications for stratigraphic correlations, *in* IX Simposio Bolivariano de Exploracion Petrolera en las Cuencas Subandinas: Cartagena, Colombia Asociación Colombiana de Geólogos y Geofísicos del Petróleo, 13 p.

Benavides, C., 2004, Estudio Mineralogico sobre Ripios secos Gibraltar 2: Informe final para Ecopetrol-AEX: Bucaramanga, Instituto Colombiana del Petróleo ICP (internal report), 15 p.

Bodine, J.H., 1981, Numerical Computation of Plate Flexure in Marine Geophysics: Lamont-Doherty Geological Observatory of Columbia University Technical Report 1, 153 p.

Boinet, T., Bourgois, J., Mendoza, H., and Vargas, R., 1985, Le poinçon de pamplona (Colombie): Un jalon de la frontière meridionale de la plaque Caraïbe: Bulletin de la Société Géologique de France, v. 8, p. 403–413.

Branquet, Y., Laumonier, B., Cheilletz, A., and Giuliani, G., 1999, Emeralds in the Eastern Cordillera of Colombia: Two tectonic settings for one mineralization: Geology, v. 27, p. 597–600, doi: 10.1130/0091-7613(1999)027<0597:EITECO>2.3.CO;2.

Branquet, Y., Cheilletz, A., Cobbold, P., Baby, P., Laumonier, B., and Giuliani, G., 2002, Andean deformation and rift inversion, eastern edge of the Cordillera Oriental (Guateque-Medina area), Colombia: Journal of South American Earth Sciences, v. 15, p. 391–407, doi: 10.1016/S0895-9811(02)00063-9.

Cardozo, N., and Jordan, T., 2001, Causes of spatially variable tectonic subsidence in the Miocene Bermejo foreland basin, Argentina: Basin Research, v. 13, p. 335–357, doi: 10.1046/j.0950-091x.2001.00154.x.

Casero, P., Salel, J.F., and Rossato, A., 1997, Multidisciplinary correlative evidences for polyphase geological evolution of the foothills of the Cordillera Oriental (Colombia), *in* VI Simposio Bolivariano de Exploración Petrolera en las Cuencas Subandinas: Cartagena, Colombia, Asociación Colombiana de Geólogos y Geofísicos del Petróleo, p. 100–118.

Cazier, E.C., Hayward, A.B., Espinosa, G., Velandia, J., Mugniot, J.F., and Leel, W.G., 1995, Petroleum geology of the Cusiana field, Llanos Basin foothills, Colombia: The American Association of Petroleum Geologists Bulletin, v. 79, p. 1444–1463.

Cediel, F., and Cáceres, C., 1988, Geologic Map of Colombia: Bogotá, Geotec Ltd., scale 1:1,200,000.

Cediel, F., Shaw, R., and Cáceres, C., 2003, Tectonic assembly of the Northern Andean block, *in* Bartolini, C., Buffler, R., and Blickwede, J., eds., The Circum-Gulf of Mexico and the Caribbean: Hydrocarbon Habitats, Basin Formation and Plate Tectonics: American Association of Petroleum Geologists Memoir 79, p. 815–848.

Céspedes, S., and Peña, L., 1995, Relaciones Estratigráficas y Ambientes de Depósito de las Formaciones del Terciario Inferior Aflorante entre Tunja y Paz del Rio, Boyacá. [Undergraduate thesis]: Bogotá, Universidad Nacional de Colombia, 50 p.

Chigne, N., Loureiro, D., and Rojas, E., 1997, El piedemonte de la Cordillera Oriental de Colombia y de los Andes de Merida; estilos estructurales y consideraciones sobre la génesis y migración de hidrocarburos, *in* VI Simposio Bolivariano de Exploración Petrolera en las Cuencas Subandinas: Cartagena, Asociación Colombiana de Geólogos y Geofísicos del Petróleo, p. 457–477.

Colleta, B., Hébrard, F., Letouzey, J., Werner, P., and Rudkiewikz, J.L., 1990, Tectonic style and crustal structure of the Eastern Cordillera (Colombia), from a balanced cross section, *in* Letouzey, J., ed., Petroleum and Tectonics in Mobile Belts: Paris, Editions Technip, p. 81–100.

Colmenares, F., 1993, Columnas estratigráficas en el Piedemonte Llanero para la BP-Colombia: Bogotá, Internal report, scale 1:100.

Cooper, M.A., Addison, F.T., Alvarez, R., Coral, M., Graham, R.H., Hayward, A.B., Howe, S., Martinez, J., Naar, J., Peñas, R., Pulham, A.J., and Taborda, A., 1995, Basin development and tectonic history of the Llanos Basin, Eastern Cordillera, and middle Magdalena Valley, Colombia: The American Association of Petroleum Geologists Bulletin, v. 79, p. 1421–1443.

Corredor, F., 2003, Eastward extent of the late Eocene–early Oligocene onset of deformation across the northern Andes: Constraints from the northern portion of the Eastern Cordillera fold belt, Colombia: Journal of South American Earth Sciences, v. 16, p. 445–457, doi: 10.1016/j.jsames.2003.06.002.

Cortés, M., Aristizabal, J.J., Bayona, G., Ojeda, G., Reyes, A., and Gamba, N., 2006a, Structure and kinematics of the Eastern foothills of the Eastern Cordillera of Colombia from balanced cross-sections and forward modelling, *in* IX Simposio Bolivariano de Exploracion Petrolera en las Cuencas Subandinas: Cartagena, Colombia, Asociación Colombiana de Geólogos y Geofísicos del Petróleo, 14 p.

Cortés, M., Colleta, B., and Angelier, J., 2006b, Structure and tectonics of the central segment of the Eastern Cordillera of Colombia: Journal of South American Earth Sciences, v. 21, p. 437–465, doi: 10.1016/j.jsames.2006.07.004.

DeCelles, P., and Giles, K., 1996, Foreland basin systems: Basin Research, v. 8, p. 105–123, doi: 10.1046/j.1365-2117.1996.01491.x.

Dengo, C.A., and Covey, M.C., 1993, Structure of the Eastern Cordillera of Colombia: Implications for trap styles and regional tectonics: The American Association of Petroleum Geologists Bulletin, v. 77, p. 1315–1337.

Diaz, L., 1994, Reconstruccion de la cuenca del Valle superior del Magdalena, a finales del Cretacico, *in* Etayo-Serna, F., ed., Estudios Geológicos del Valle Superior del Magdalena: Bogotá, Universidad Nacional de Colombia, p. 13, Chapter XI.

Etayo-Serna, F., Barrero, D., Lozano, H., and 15 others, 1983, Mapa de Terrenos Geológicos de Colombia, Publicación Geológica Especial: Bogotá, Ingeominas, 235 p.

Fabre, A., 1981, Estratigrafía de la Sierra Nevada del Cocuy, Boyacá y Arauca, Cordillera Oriental (Colombia): Geología Norandina, v. 4, p. 3–12.

Fabre, A., 1987, Tectonique et géneration d'hydrocarbures: Un modèle de l'evolution de la Cordillère Orientale de Colombie et du Bassin de Llanos pendant le Crétacé et le Tertiaire: Archives des Sciences Genève, v. 40, p. 145–190.

Fajardo, A., 1995, 4-D Stratigraphic Architecture and 3-D Reservoir Fluid-Flow Model of the Mirador Formation, Cusiana Field, Foothills Area of the Cordillera Oriental, Colombia [Master's thesis]: Golden, Colorado School of Mines, 171 p.

Fajardo, A., Rojas, E., Cristancho, J., and Consorcio G&G Going System, 2000, Definición del Modelo estratigrafico en el Intervalo Cretaceo Tardio a Mioceno Medio en la Cuenca Llanos Orientales y Piedemonte Llanero: Informe Final: Bucaramanga, Ecopetrol S.A. y Instituto Colombiano del Petroleo, 181 p.

Fajardo-Peña, G., 1998, Structural Analysis and Basin Inversion Evolutionary Model of the Arcabuco, Tunja and Sogamoso Regions, Eastern Cordillera, Colombia [M.Sc. thesis]: Boulder, University of Colorado, 114 p.

Flemings, P.B., and Jordan, T.E., 1990, Stratigraphic modelling of foreland basins: Interpreting thrust deformation and lithosphere rheology: Geology, v. 18, p. 430–434, doi: 10.1130/0091-7613(1990)018<0430:SMOFBI>2.3.CO;2.

Geoconsult-Pangea, 2003, Consultoria para el Desarrollo de Actividades que Conduzcan a Reducir el Riesgo Exploratorio en el Piedemoente Llanero—Proyecto Flujo Regional de Fluidos: Bucaramanga, Reporte Interno Ecopetrol-ICP.

Geoestratos-Dunia, 2003, Control Geológico de Campo del Bloque Sirirí y Áreas Aledañas: Informe Final: Bucaramanga, Ecopetrol S.A. y Instituto Colombiano del Petroleo, 181 p.

George, R., Pindell, J., and Cristancho, J., 1997, Eocene paleostructure of Colombia and implications for history of generation and migration of hydrocarbons, *in* VI Simposio Bolivariano de Exploración Petrolera en las Cuencas Subandinas: Cartagena, Colombia, Asociación Colombiana de Geólogos y Geofísicos del Petróleo, p. 133–140.

Gómez, E., Jordan, T., Allmendinger, R.W., Hegarty, K., Kelley, S., and Heizler, M., 2003, Controls on architecture of the Late Cretaceous to Cenozoic southern Middle Magdalena Valley Basin: Geological Society of America Bulletin, v. 115, p. 131–147, doi: 10.1130/0016-7606(2003)115<0131:COAOTL>2.0.CO;2.

Gómez, E., Jordan, T., Allmendinger, R.W., and Cardozo, N., 2005a, Development of the Colombian foreland-basin system as a consequence of diachronous exhumation of the northern Andes: Geological Society of America Bulletin, v. 117, p. 1272–1292, doi: 10.1130/B25456.1

Gómez, E., Jordan, T., Allmendinger, R.W., Hegarty, K., and Kelley, S., 2005b, Syntectonic Cenozoic sedimentation in the northern middle Magdalena Valley Basin of Colombia and implications for exhumation of the northern Andes: Geological Society of America Bulletin, v. 117, no. 5/6, p. 547–569, doi: 10.1130/B25454.1

Guerrero, J., and Sarmiento, G., 1996, Estratigrafía física, palinológica, sedimentológica y secuencial del Cretácico Superior y Paleoceno del Piedemonte Llanero: Implicaciones en exploración petrolera: Geologia Colombiana, v. 20, p. 3–66.

Haq, B.U., Hardenbol, J., and Vail, P., 1987, Chronology of fluctuating sea levels since the Triassic: Science, v. 235, p. 1156–1166, doi: 10.1126/science.235.4793.1156.

Helmens, K.F., 1990, Neogene–Quaternary geology of the high plain of Bogotá, Eastern Cordillera, Colombia (stratigraphy, paleoenvironments and landscape evolution): Berlin, Gebruder Borntraeger Verlagsbuchhandlung, Dissertationes Botanicae, 202 p.

Helmens, K.F., and Van der Hammen, T., 1994, The Pliocene and Quaternary of the high plain of Bogotá (Colombia): A history of tectonic uplift, basic development and climatic change: Quaternary International, v. 21, p. 41–61, doi: 10.1016/1040-6182(94)90020-5.

Herrera, F., 2004, Paleotemperatura y Paleoprecipitación del Paleoceno Superior en Zonas Tropicales usando Plantas Megafósiles de la Fm. Cerrejón [Undergraduate thesis]: Bucaramanga, Universidad Industrial de Santander, 44 p.

Hooghiemstra, H., and Van der Hammen, T., 1998, Neogene and Quaternary development of the neotropical rain forest: The forest refugia hypothesis, and a literature overview: Earth-Science Reviews, v. 44, p. 147–183, doi: 10.1016/S0012-8252(98)00027-0.

Hoorn, C., 1988, Quebrada del Mochuelo, Type Locality of the Bogotá Formation: A Sedimentological, Petrographical and Palynological Study: Hugo de Vries Laboratory: Amsterdam, University of Amsterdam, 21 p.

Hoorn, C., 1994, Fluvial palaeoenvironments in the Amazonas Basin (early Miocene to early middle Miocene, Colombia): Palaeoclimatology, Palaeogeography, Palaeoecology, v. 109, p. 1–54, doi: 10.1016/0031-0182(94)90117-1.

Hoorn, C., Guerrero, J., Sarmiento, G.A., and Lorente, M.A., 1995, Andean tectonics as a cause for changing drainage patterns in Miocene northern South America: Geology, v. 23, p. 237–240, doi: 10.1130/0091-7613(1995)023<0237:ATAACF>2.3.CO;2.

Horton, B.K., 1999, Erosional control on the geometry and kinematics of thrust belt development in the central Andes: Tectonics, v. 18, p. 1292–1304, doi: 10.1029/1999TC900051.

Horton, B.K., Hampton, B.A., and Waanders, G.L., 2001, Paleogene synorogenic sedimentation in the Altiplano plateau and implications for initial mountain building in the Central Andes: Geological Society of America Bulletin, v. 113, no. 11, p. 1387–1400, doi: 10.1130/0016-7606(2001)113<1387:PSSITA>2.0.CO;2.

Hossack, J., Martinez, J., Estrada, C., and Herbert, R., 1999, Structural evolution of the Llanos fold and thrust belt, Colombia, *in* McClay, K., ed., Thrust Tectonics 99 Meeting: London, Royal Halloway University of London, p. 110.

Jaramillo, C., 1999, Middle Paleogene Palynology of Colombia, South America: Biostratigraphic, Sequence Stratigraphic and Diversity Implications [Ph.D. thesis]: Gainsville, University of Florida, 416 p.

Jaramillo, C., and Dilcher, D.L., 2001, Middle Paleogene palynology of central Colombia, South America: A study of pollen and spores from tropical latitudes: Palaeontographica B, v. 258, p. 87–213.

Jaramillo, C., Rueda, M., and Mora, G., 2006a, Cenozoic plant diversity in the neotropics: Science, v. 311, p. 1893–1896, doi: 10.1126/science.1121380.

Jaramillo, C., Rueda, M., Torres, V., Parra, F., Rodriguez, G., Bedoya, G., Santos, C., Vargas, C., and Mora, G., 2006b, Palinología del Paleógeno del Norte de Suramérica: Un acercamiento a la cronoestratigrafía de las Cuencas del Piedemonte y Llanos de Colombia, *in* IX Simposio Bolivariano de Exploracion Petrolera en las Cuencas Subandinas: Cartagena, Colombia, Asociación Colombiana de Geólogos y Geofísicos del Petróleo, 8 p.

Johnsson, M.J., Stallard, R.F., and Lundberg, N., 1991, Controls on the composition of fluvial sands from a tropical weathering environment: Sands of the Orinoco River drainage basin, Venezuela and Colombia: Geological Society of America Bulletin, v. 103, p. 1622–1647, doi: 10.1130/0016-7606(1991)103<1622:COTCOF>2.3.CO;2.

Jordan, T.E., 1981, Thrust loads and foreland basin evolution, Cretaceous, western United States: The American Association of Petroleum Geologists Bulletin, v. 65, p. 2506–2520.

Julivert, M., 1963, Los rasgos tectónicos de la Sabana de Bogotá y los mecanísmos de formación de las estructuras: Boletin Geológico Universidad Industrial de Santander, v. 13–14, p. 5–102.

Kammer, A., and Sanchez, J., 2006, Early Jurassic rift structures associated with the Soapaga and Boyacá faults of the Eastern Cordillera, Colombia: Sedimentological inferences and regional implications: Journal of South American Earth Sciences, v. 21, p. 412–422, doi: 10.1016/j.jsames.2006.07.006.

Kohn, B.P., Shagam, R., Banks, P.O., and Burkley, E.A., 1984, Mesozoic-Pleistocene fission track ages on rocks of the Venezuela Andes and their tectonic implications, *in* Bonini, W.E., Hargraves, R.B., and Shagam, R., eds., The Caribbean–South American Plate Boundary and Regional Tectonics: Geological Society of America Memoir 162, p. 365–384.

Liu, S., Nummedal, D., Yin, P., and Luo, H., 2005, Linkage of Sevier thrusting episodes and Late Cretaceous foreland basin megasequences across southern Wyoming (USA): Basin Research, v. 17, p. 487–506, doi: 10.1111/j.1365-2117.2005.00277.x.

Macedo, J., and Marshak, S., 1999, Controls on the geometry of fold-thrust belt salients: Geological Society of America Bulletin, v. 111, p. 1808–1822, doi: 10.1130/0016-7606(1999)111<1808:COTGOF>2.3.CO;2.

Martinez, J., 2006, Structural evolution of the Llanos foothills, Eastern Cordillera, Colombia: Journal of South American Earth Sciences, v. 21, p. 510–520, doi: 10.1016/j.jsames.2006.07.010.

McCourt, W.J., Feininger, T., and Brook, M., 1984, New geological and geochronological data from the Colombian Andes: Continental growth by multiple accretion: Journal of the Geological Society of London, v. 141, p. 831–845, doi: 10.1144/gsjgs.141.5.0831.

Mesa, A., 1997, Diagenesis and Reservoir Quality of the Guadalupe, Barco and Mirador Formations (Campanian to Eocene), Llanos Basin, Colombia [Ph.D. thesis]: Mainz, Johannes Gutenberg Universitat, 141 p.

Mesa, A., 2004, Descripcion Detallada Petrografica del Pozo Gibraltar 2: Informe Final: Bucaramanga, Ecopetrol S.A. y Instituto Colombiano del Petroleo, 28 p.

Mora, A., and Parra, M., 2004, Secciones Estratigraficas de las Formaciones Guadalupe, Barco y Carbonera, Anticlinal del Guavio: Informe Final: Bucaramanga, Instituto Colombiano del Petroleo, 28 p.

Mora, A., Parra, M., Strecker, M.R., and Sobel, E., 2005, Influences of tectonic inheritance and exhumation patterns in the timing and structural styles of the Eastern Cordillera of Colombia, *in* Sixth International Symposium of Andean Geodynamics, Extended abstract: Barcelona, Institut de Recherche pour le Developpement, p. 524–526.

Mora, A., Parra, M., Strecker, M.R., Kammer, A., Dimate, C., and Rodriguez, F., 2006, Cenozoic contractional reactivation of Mesozoic extensional structures in the Eastern Cordillera of Colombia: Tectonics, v. 25, p. TC2010, doi: 10.1029/2005TC001854

Moreno, J., and Velasquez, M., 1993, Estratigrafía y Tectónica en los Alrededores del Municipio de Nuchia Departamento de Casanare, Colombia [Undergraduate thesis]: Bogotá, Universidad Nacional de Colombia, 75 p.

Narr, W., and Suppe, J., 1994, Kinematics of basement-involved compressive structures: American Journal of Science, v. 294, p. 802–860.

Ojeda, G., 2000, Analysis of Flexural Isostasy of the Northern Andes [PH.D. thesis]: Miami, Florida International University, 96 p.

Ojeda, G., and Whitman, D., 2002, Effect of windowing on lithosphere elastic thickness estimates obtained via the coherence method: Results from northern South America: Journal of Geophysical Research, v. 107, no. B11, 2275, doi: 10.1029/2000jb000114.

Pardo-Trujillo, A., 2004, Paleocene-Eocene Palynology and Palynofacies from Northeastern Colombia and Western Venezuela [Ph.D. thesis]: Leige, Université de Liege, 103 p.

Pardo-Trujillo, A., Jaramillo, C., and Oboh-Ikuenobe, F., 2003, Paleogene Palynostratigraphy of the Eastern middle Magdalena Valley: Palynology, v. 27, p. 155–178, doi: 10.2113/27.1.155.

Parra, M., Mora, A., Jaramillo, C., Strecker, M.R., and Veloza, G., 2005, New stratigraphic data on the initiation of mountain building at the eastern front of the Colombian Eastern Cordillera, *in* 6th International Symposium on Andean Geodynamics, Extended Abstracts: Barcelona, Insitut de Recherche pour le Developpement, p. 567–571.

Perez, G., and Salazar, A., 1978, Estratigrafia y facies del Grupo Guadalupe: Geologia Colombiana, v. 10, p. 7–85.

Pindell, J.L., Higgs, R., and Dewey, J., 1998, Cenozoic palinspastic reconstruction, paleogeographic evolution and hydrocarbon setting of the northern margin of South America, *in* Pindell, J., and Drake, C., eds., Paleogeographic Evolution and Non-Glacial Eustasy, Northern South America: Society for Sedimentary Geology Special Publication 58, p. 45–84.

Pindell, J.L., Kennan, L., Maresch, W.V., Stanek, K.-P., Draper, G., and Higgs, R., 2005, Plate kinematics and crustal dynamics of circum-Caribbean arc-continent interactions: Tectonic controls on basin development in proto-Caribbean margins, *in* Avé-Lallemant, H.G., and Sisson, V.B., eds., Caribbean-South American Plate Interactions, Venezuela: Geological Society of America Special Paper 394, p. 7–52.

Pulham, A.J., Mitchell, A., MacDonald, D., and Daly, C., 1997, Reservoir modeling in the Cusiana field, Llanos foothills, Eastern Cordillera: Characterization of a deeply-buried, low-porosity reservoir, *in* VI Simposio Bolivariano de Exploracion Petrolera en las Cuencas Subandinas: Cartagena, Colombia, Asociación Colombiana de Geólogos y Geofísicos del Petróleo, p. 198–216.

Rathke, W.W., and Coral, M., 1997, Cupiagua field, Colombia: Interpretation case history of a large, complex thrust belt gas condensate field, *in* VI Simposio Bolivariano de Exploracion Petrolera en las Cuencas Subandinas: Cartagena, Colombia, Asociación Colombiana de Geólogos y Geofísicos del Petróleo, p. 119–128.

Restrepo-Pace, P., Colmenares, F., Higuera, C., and Mayorga, M., 2004, A fold-and-thrust belt along the western flank of the Eastern Cordillera of Colombia—Style, kinematics, and timing constraints derived from seismic data and detailed surface mapping, *in* McClay, K., ed., Thrust Tectonics and Hydrocarbon Systems: American Association of Petroleum Geologists Memoir 82, p. 598–613.

Reyes, A., 1996, Sedimentology and Stratigraphy and Its Control on Porosity and Permeability Barco Formation, Cusiana Field, Colombia [Master's thesis]: Reading, University of Reading, 70 p.

Reyes, A., 2004, Taller Corazon Gibraltar-2: Bucaramanga, Reporte Interno Ecopetrol, 12 p.

Reyes, I., and Valentino, M. T., 1976, Geologia del yacimiento y variabilidad de las caracteristicas geoquimicas del mineral de hierro en la region de Paz Vieja (Municipio de Paz del Rıo, Departamento de Boyaca): Bogotá, Primer Congreso Colombiano de Geologia, Memorias: p. 267–324.

Rochat, P., Rosero, A., Gonzalez, R., Florez, I., Lozada, M., and Petton, R., 2003, Thrust kinematics of the Tangara/Mundonuevo area: New insight from apatite fission track analysis, *in* VIII Simposio Bolivariano de Exploración Petrolera en las Cuencas Subandinas: Cartagena, Colombia, Asociación Colombiana de Geólogos y Geofíscos del Petróleo, p. 147–154.

Roeder, D., and Chamberlain, R.L., 1995, Eastern Cordillera of Colombia: Jurassic Neogene crustal evolution, *in* Tankard, A.J., Suarez, R., and Welsink, H.J. eds., Petroleum Basins of South America: American Association of Petroleum Geologists Memoir 62, p. 633–645.

Rowan, M., and Linares, R., 2000, Fold-evolution matrices and axial-surface analysis of fault-bend folds: Application to the Medina anticline, Eastern Cordillera, Colombia: The American Association of Petroleum Geologists Bulletin, v. 84, p. 741–764.

Royero, J. M., 2001, Geología y geoquímicas de la Plancha Toledo 111–Norte de Santander, Escala 1:100,000: Memoria Explicativa: Ingeominas, 53 p.

Sarmiento, G., 1992, Estratigrafía y Medio de Depósito de la Formación Guaduas: Boletín Geológico Ingeominas, v. 32, no. 1–3, p. 3–44.

Sarmiento-Rojas, L.F., 2001, Mesozoic Rifting and Cenozoic Basin Inversion History of the Eastern Cordillera, Colombian Andes; Inferences from Tectonic Models: Bogotá, Ecopetrol y Netherlands Research School of Sedimentary Geology, 295 p.

Sarmiento-Rojas, L.F., Van Wess, J.D., and Cloetingh, S., 2006, Mesozoic transtensional basin history of the Eastern Cordillera, Colombian Andes: Inferences from tectonic models: Journal of South American Earth Sciences, v. 21, p. 383–411, doi: 10.1016/j.jsames.2006.07.003.

Shagam, R., Kohn, B.P., Banks, P.O., Dasch, L.E., Vargas, R., Rodriguez, G.I., and Pimentel, N., 1984, Tectonic implications of Cretaceous-Pliocene fission-track ages from rocks of the circum–Maracaibo Basin region of western Venezuela and eastern Colombia, *in* Bonini, W.E., Hargraves, R.B., and Shagam, R., eds., The Caribbean-South American Plate Boundary and Regional Tectonics: Geological Society of America Memoir 162, p. 385–412.

Stewart, J., and Watts, A.B., 1997, Gravity anomalies and spatial variations of flexural rigidity at mountain ranges: Journal of Geophysical Research, v. 102, p. 5327–5352, doi: 10.1029/96JB03664.

Taboada, A., Rivera, L.A., Fuenzalida, A., Cisternas, A., Philip, H., Bijwaard, H., Olaya, J., and Rivera, C., 2000, Geodynamics of the northern Andes: Subductions and intracontinetal deformation (Colombia): Tectonics, v. 19, no. 5, p. 787–813, doi: 10.1029/2000TC900004.

Toro, G., 1999, Chronology of the volcanic activity and regional thermal events: A contribution from the tephrochronology in the north of the Central Cordillera Colombia, *in* 4th International Symposium on Andean Geodynamics: Göttingen, Germany, Institut de Recherche pour le Developpement, p. 761–763.

Toro, J., 1990, The Termination of the Bucaramanga Fault in the Cordillera Oriental, Colombia [M.Sc. thesis]: Tucson, University of Arizona, 60 p.

Toro, J., Roure, F., Bordas-Le Flonch, N., Le Cornec-Lance, S., and Sassi, W., 2004, Thermal and kinematic evolution of the Eastern Cordillera fold and thrust belt, Colombia, *in* Swennen, R., Roure, F., and Granath, J. W., eds., Deformation, Fluid Flow, and Reservoir Appraisal in Foreland Fold and Thrust Belts: American Association of Petroleum Geologists Hedberg Series, no. 1, p. 79– 115.

Torres, J., 2003, Caracterización Petrográfica de la Discordancia Pre-Eocénica en el Area de la Sabana de Bogotá [Undergraduate thesis]: Bogotá, Universidad Nacional de Colombia, 88 p.

Van der Wiel, A.M., 1991, Uplift and Volcanism of the SE Colombian Andes in Relation to Neogene Sedimentation of the Upper Magdalena Valley [Ph.D. thesis]: Wageningen, Free University, 208 p.

Vasquez, C., 1983, Geología del Paleoceno Superior en la Margen Occidental de la Cuenca de Los Llanos Orientales [Undergraduate thesis]: Bogotá, Universidad Nacional de Colombia, 162 p.

Villamil, T., 1999, Campanian-Miocene tectonostratigraphy, depocenter evolution and basin development of Colombia and western Venezuela: Palaeogeography, Palaeoclimatology, Palaeoecology, v. 153, p. 239–275, doi: 10.1016/S0031-0182(99)00075-9.

Villamil, T., Arango, C., Suarez, M., Malagon, C., and Linares, R., 1995, Discordancia Paleoceno-Eoceno y depositios sobreyacentes en Colombia: Implicaciones tectonicas y de geologia del Petroleo, *in* VI Congreso Colombiano del Petroleo: Bogotá, Asociación Colombiana de Geólogos y Geofísicos del Petróleo, p. 11–16.

Villamil, T., Muñoz, J., Sanchez, J., Aristizabal, J.J., Velasco, J., Luna, P.E., Mantilla, A., Fajardo, A., Peña, L.E., Paz, M.G., Silva, O., Sanchez, E., and Meza, N., 2004, The Gibraltar discovery, northern Llanos foothills, Colombia: Case history of an exploration success in a frontier area: Journal of Petroleum Geology, v. 27, no. 4, p. 321–334, doi: 10.1111/j.1747-5457.2004.tb00061.x.

Warren, E.A., and Pulham, A.J., 2001, Anomalous porosity and permeability preservation in deeply buried Tertiary and Mesozoic sandstones in the Cusiana field, Llanos foothills, Colombia: Journal of Sedimentary Research, v. 71, p. 2–14, doi: 10.1306/081799710002.

Watts, A.B., 2001, Isostasy and Flexure of the Lithosphere: Cambridge, UK, Cambridge University Press, 458 p.

Watts, A.B., and Ryan, W.B., 1976, Flexure of the lithosphere and continental margin basins: Tectonophysics, v. 36, p. 25–44, doi: 10.1016/0040-1951(76)90004-4.

Yepes, O., 2001, Maastrichtian-Danian dinoflagellate cyst biostratigraphy and biogeography from two equatorial sections in Colombia and Venezuela: Palynology, v. 25, p. 217–249, doi: 10.2113/0250217.

Manuscript received 26 January 2007
Revised manuscript received 23 November 2007
Manuscript accepted 27 December 2007

Printed in the USA